Article

Cell Reports

CD4+ T Follicular Helper Cells in Human Tonsils and Blood Are Clonally Convergent but Divergent from Non-Tfh CD4+ Cells

Graphical Abstract

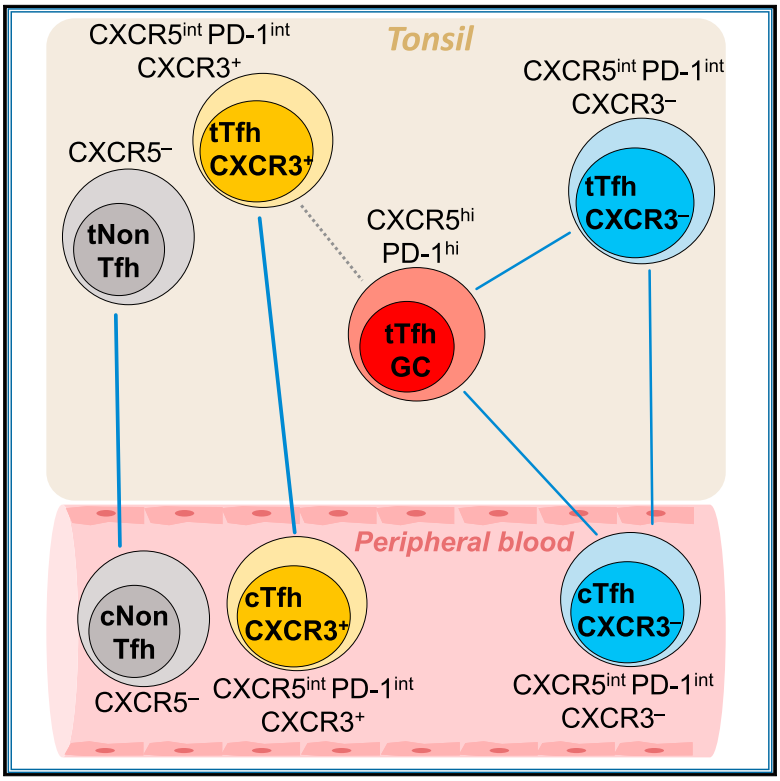

Highlights

- The blood and tonsil CD4+ T follicular helper (Tfh) repertoires overlap extensively
- Dominant Tfh clonotypes differ from those of non-Tfh, which predominate in blood
- Influenza-specific Tfh and non-Tfh clones exhibit repertoire differences
- Influenza-specific Tfh clones in blood are found in the tonsil CXCR3+Tfh subset

Authors

Elena Brenna, Alexey N. Davydov, Kristin Ladell, ..., Dmitriy M. Chudakov, Persephone Borrow, Andrew J. McMichael

Correspondence

elena.brenna@ndm.ox.ac.uk (E.B.), persephone.borrow@ndm.ox.ac.uk (P.B.), andrew.mcmichael@ndm.ox.ac.uk (A.J.M.)

In Brief

CD4+ T follicular helper (Tfh) cells are fundamental for antibody production. Brenna et al. demonstrate extensive repertoire overlap between Tfh populations in human blood and tonsils, whereas non-Tfh repertoires differ profoundly. Therefore, analysis of Tfh but not of total circulating CD4+ T cells can reflect the specificity of lymphoid tissue Tfh cells.

Brenna et al., 2020, Cell Reports *30*, 137–152
January 7, 2020
https://doi.org/10.1016/j.celrep.2019.12.016

CellPress

Cell Reports
Article

CD4+ T Follicular Helper Cells in Human Tonsils and Blood Are Clonally Convergent but Divergent from Non-Tfh CD4+ Cells

Elena Brenna,[1,*] Alexey N. Davydov,[2] Kristin Ladell,[3] James E. McLaren,[3] Paolo Bonaiuti,[4] Maria Metsger,[2] James D. Ramsden,[5] Sarah C. Gilbert,[6] Teresa Lambe,[6] David A. Price,[3,7] Suzanne L. Campion,[1] Dmitriy M. Chudakov,[2,8,9] Persephone Borrow,[1,10,*] and Andrew J. McMichael[1,10,11,*]

[1]Nuffield Department of Clinical Medicine, University of Oxford, Oxford OX3 7FZ, UK
[2]Central European Institute of Technology, Brno 601 77, Czech Republic
[3]Division of Infection and Immunity, Cardiff University School of Medicine, Cardiff CF14 4XN, UK
[4]Istituto Firc di Oncologia Molecolare, Milano 20139, Italy
[5]West Wing ENT, John Radcliffe Hospital, Oxford OX3 9DU, UK
[6]The Jenner Institute, University of Oxford, Oxford OX3 7DQ, UK
[7]Systems Immunity Research Institute, Cardiff University School of Medicine, Cardiff CF14 4XN, UK
[8]Center for Precision Genome Editing and Genetic Technologies for Biomedicine, Pirogov Russian National Research Medical University, Moscow 117997, Russia
[9]Shemyakin-Ovchinnikov Institute of Bioorganic Chemistry, Russian Academy of Science, Moscow 117997, Russia
[10]These authors contributed equally
[11]Lead Contact
*Correspondence: elena.brenna@ndm.ox.ac.uk (E.B.), persephone.borrow@ndm.ox.ac.uk (P.B.), andrew.mcmichael@ndm.ox.ac.uk (A.J.M.)
https://doi.org/10.1016/j.celrep.2019.12.016

SUMMARY

T follicular helper (Tfh) cells are fundamental for B cell selection and antibody maturation in germinal centers. Circulating Tfh (cTfh) cells constitute a minor proportion of the CD4+ T cells in peripheral blood, but their clonotypic relationship to Tfh populations resident in lymph nodes and the extent to which they differ from non-Tfh CD4+ cells have been unclear. Using donor-matched blood and tonsil samples, we investigate T cell receptor (TCR) sharing between tonsillar Tfh cells and peripheral Tfh and non-Tfh cell populations. TCR transcript sequencing reveals considerable clonal overlap between peripheral and tonsillar Tfh cell subsets as well as a clear distinction between Tfh and non-Tfh cells. Furthermore, influenza-specific cTfh cell clones derived from blood can be found in the repertoire of tonsillar Tfh cells. Therefore, human blood samples can be used to gain insight into the specificity of Tfh responses occurring in lymphoid tissues, provided that cTfh subsets are studied.

INTRODUCTION

T follicular helper (Tfh) cells are specialized CD4+ T cells primarily found in germinal centers (GCs) of secondary lymphoid organs (Breitfeld et al., 2000; Kim et al., 2001; Schaerli et al., 2000). Tfh cells play a critical role in supporting B cell responses and selection of affinity-matured antibodies (Breitfeld et al., 2000; Bryant et al., 2007; Ma et al., 2009). They mediate their effects via receptor-ligand interactions with B cells and production of cytokines such as interleukin-21 (IL-21), IL-4, and the B-cell activating factor (BAFF), which induce survival and proliferation in B cells and support antibody class switching (Avery et al., 2008; Casamayor-Palleja et al., 1995; Liu et al., 1989). Expression of the chemokine receptor CXCR5 is fundamental for migration of pre-Tfh cells to the T-B cell border in lymphoid tissues and maturation of Tfh cells into B cell follicles and GCs along the follicular CXCL13 gradient (Ansel et al., 2000; Förster et al., 1996). In addition to CXCR5, Tfh cells also express PD-1 and ICOS (inducible T-cell costimulator) (Choi et al., 2011; Dorfman et al., 2006; Haynes et al., 2007; Xu et al., 2013). Some memory CD4+ T cells in secondary lymphoid organs express intermediate levels of these markers, but Tfh cells within the GC (Tfh GC cells) express high levels of CXCR5 and PD-1; hence, a CXCR5^{hi}PD-1^{hi} phenotype is commonly used to distinguish Tfh GC cells (Shi et al., 2018). Differences in expression of these surface markers reflect the location of CD4+ T cell sub-populations and their activation, differentiation, and functional status (Crotty, 2018).

Populations of CD4+ memory T cells in the blood with similar characteristics as lymphoid Tfh cells are thought to represent circulating memory Tfh (cTfh) cells (Crotty, 2018; Hale and Ahmed, 2015). These peripheral cTfh cells express CXCR5, PD-1, and ICOS but at much lower levels than Tfh GC cells, although a minute population of circulating PD-1^{hi}CXCR5^{hi} CD4+ T cells can also be detected (He et al., 2013; Vinuesa et al., 2016). Although there is some controversy about phenotypic definition of cTfh cells, it is accepted that circulating CXCR5+CD4+ T cells promote immunoglobulin (Ig) class switching and plasmablast formation in co-culture with naive or memory B cells (Bentebibel et al., 2013; He et al., 2013; Locci et al., 2016; Morita et al., 2011). Different subsets of cTfh cells have been distinguished: Th1-like (CXCR3+CCR6−), Th2-like

(CXCR3$^-$CCR6$^-$), and Th17-like (CXCR3$^-$CCR6$^+$) cTfh cells, based on similarities with canonical Th CD4$^+$ cell subpopulations (Bentebibel et al., 2013; Morita et al., 2011). The diversity of cTfh cells is also evidenced by the differences in cytokine production and transcription factor expression observed when cTfh cell subsets are co-cultured with naive B cells in the presence of staphylococcal enterotoxin B (SEB). Th1-like subsets produce interferon γ (IFN-γ); Th2-like IL-4, IL-5, and IL-13; and Th17-like IL-17A and IL-22 (Bentebibel et al., 2013; Morita et al., 2011).

The Th2- and Th17-like subsets of cTfh cells provide better B cell help *in vitro* than Th1-like cTfh cells (Boswell et al., 2014; Locci et al., 2013; Morita et al., 2011), and the transcriptional profile of CXCR3$^-$ cTfh cells shares a strong similarity with Tfh GC cells (Locci et al., 2013). In influenza virus infection, the human CD4$^+$ T cell response is highly Th1-biased, and Th1-like (CXCR3$^+$) cTfh cells help B cells produce virus-specific antibodies (Bentebibel et al., 2013; Pallikkuth et al., 2012). However, stimulation of Th1-like Tfh effector cells after infection or vaccination is associated with an inferior GC response and suboptimal antibody production (Bowyer et al., 2018; Cubas et al., 2015; Obeng-Adjei et al., 2015; Ryg-Cornejo et al., 2016).

Difficulties in sampling secondary lymphoid organs in humans have hampered direct comparison of lymphoid and peripheral Tfh cell populations. Furthermore, the ontogeny of memory cTfh cells and their relationship with effector Tfh GC cells are still poorly understood. Although the phenotype (Chevalier et al., 2011; He et al., 2013) and transcriptional profile (Heit et al., 2017; Locci et al., 2013) of cTfh cell populations have been compared with Tfh GC cells, the extent of clonal convergence between these populations has not been fully explored. Phenotype and function are plastic features of CD4$^+$ T cells, influenced by environmental stimuli, so the same cell type can show a different phenotypic profile in different compartments or under different cell culture conditions (Sallusto et al., 2018). It has been unclear whether cTfh cells originate from CXCR5$^-$ memory CD4$^+$ T cells or from lymphoid tissue pre-Tfh or Tfh GC cells or whether they comprise a distinct lineage. Understanding the relationship between Tfh and non-Tfh cell populations in the blood and lymphoid tissues is very important for human studies, which typically investigate only peripheral blood because of the practical, ethical, and consensual barriers to accessing lymphoid tissues.

The T cell receptor (TCR) is a fixed marker of clonotype. In this study, donor-matched tonsils and peripheral blood were collected from adult volunteers undergoing tonsillectomy, and the TCR repertoires of Tfh and non-Tfh cell subsets were determined. Considerable overlap was found between peripheral and tonsillar Tfh cells and a complete disparity between Tfh cells and CXCR5$^-$ memory CD4$^+$ T cells. In addition, memory Tfh and non-Tfh cells from blood reactive with the hemagglutinin (HA) protein from influenza virus were studied (Alam and Sant, 2011; Fazilleau et al., 2007; Sant et al., 2018). HA-specific CD4$^+$ memory T cells were enriched in CXCR3$^+$ cTfh cells, and HA-specific cTfh cell clones could be found in the tonsillar CXCR3$^+$ Tfh population, confirming the clonotypic overlap between peripheral and tonsillar Tfh cell populations in an antigen-specific context. Thus, human blood samples, which are readily accessible, can be used to gain insight into the specificity of Tfh cell responses occurring in GCs, but only when cTfh cell populations are analyzed.

RESULTS

Identification of Tonsillar and Circulating Tfh Populations in Donor-Matched Samples

Matched peripheral blood and tonsil samples from adult donors were studied to compare cTfh and tonsillar Tfh (tTfh) cell populations. Multi-parameter flow cytometry-based characterization of CD4$^+$ memory T cell populations in peripheral blood mononuclear cells (PBMCs) and mononuclear cells from tonsils (MNC-Ts) was performed (Figure 1). We refer to all antigen-experienced (CD4$^+$CD45RA$^-$) cells as memory cells, although this definition encompasses central memory and effector memory/effector T cells, which we did not distinguish in this study. Expression of the Tfh markers CXCR5, PD-1, and ICOS and the chemokine receptor CXCR3 on CD4$^+$CD45RA$^-$ memory T cells (identified as shown in Figure S1A) was evaluated (Figure 1A). A population with high expression of PD-1 and CXCR5 was observed only in tonsils and was not present in appreciable numbers in peripheral blood samples. CXCR3 and ICOS were also differently expressed among blood and tonsil CD4$^+$ memory T cells (Figure 1B). In tonsils, populations with lower expression of CXCR5 and PD-1 had the highest proportion of CXCR3$^+$ cells, whereas in blood, no significant difference was observed between CXCR5$^{+/-}$ and PD-1$^{+/-}$ subsets. In contrast, ICOS was maximally expressed in tonsil and blood populations with high expression of CXCR5 and PD-1, and it decreased as these two markers declined.

Subsets of CD4$^+$ memory T cells were chosen for comparison based on the phenotypic observations made here and in prior studies (Boswell et al., 2014; Morita et al., 2011; Figure 1C). Within the CD4$^+$CD45RA$^-$ population, cTfh CXCR3$^+$ and cTfh CXCR3$^-$ subsets of CXCR5$^+$PD-1$^+$ cells and cNon-Tfh cells (CXCR5$^-$) were identified in peripheral blood. In tonsils, tTfh GC cells were identified as PD-1^{hi}CXCR5^{hi}, in contrast to the intermediate level PD-1^{int}CXCR5^{int} population, in which tTfh CXCR3$^+$ and tTfh CXCR3$^-$ cells were characterized, and tNon-Tfh (CXCR5$^-$PD-1$^-$) cells were also studied. Gates were set based on the expression of PD-1, CXCR5, and CXCR3 in CD4$^+$CD45RA$^+$ naive-enriched T cells (Figure S1B). Because PD-1 is often expressed by exhausted peripheral T cells and in Th17 CD4$^+$ cells (Aschenbrenner et al., 2018; Day et al., 2006), we did not include this marker to gate on cNon-Tfh cells from blood to ensure that we were examining the entire non-Tfh memory population. The percentage of each population within CD4$^+$CD45RA$^-$ T cells was evaluated in samples collected from 12 donors (Figure 1D). The Tfh GC subset was not found in appreciable numbers in peripheral blood, and Tfh subsets were less frequent in peripheral blood than in tonsils, whereas non-Tfh cells were more abundant.

To define the functionality of phenotypically distinct Tfh cell subsets, cytokine production from each subset was evaluated *ex vivo* after phorbol 12-myristate 13-acetate (PMA) and ionomycin stimulation, by flow cytometry. Data from 10 donors showed that Tfh GC cells were the major producers of IL-21 (Figure 1E) and IL-4 (Figure 1F), both crucial cytokines for Tfh cell differentiation and B cell survival (Nurieva et al., 2008; Reinhardt et al.,

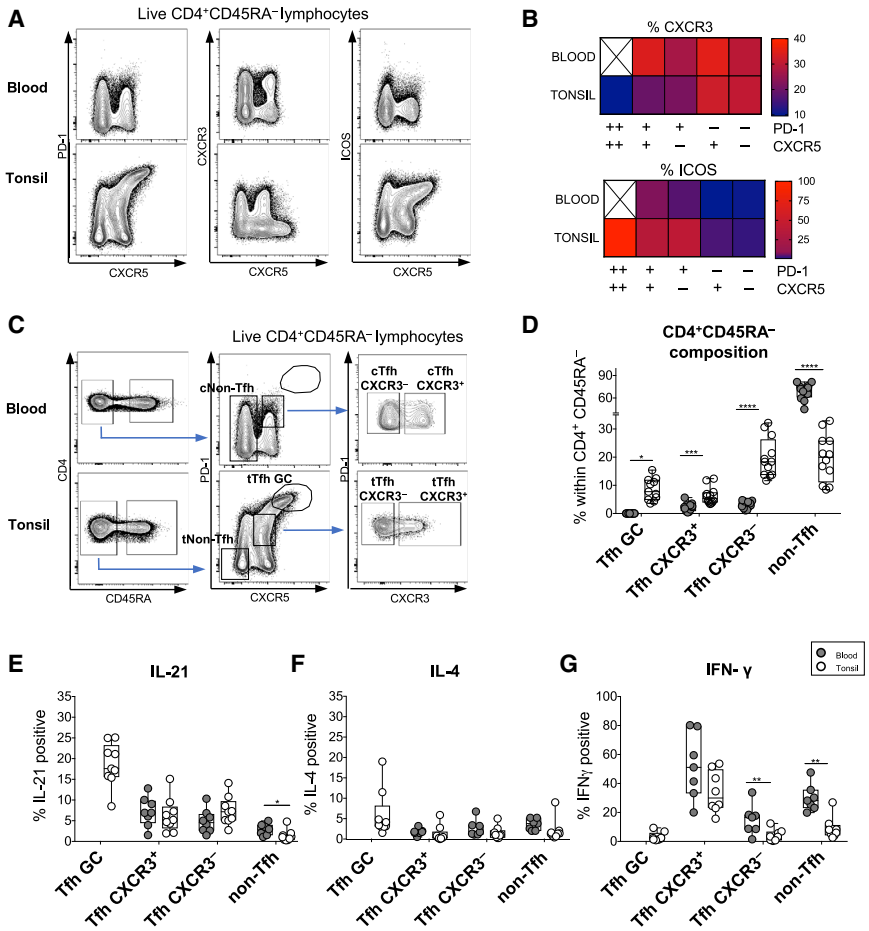

Figure 1. Identification of Tonsillar and Circulating Tfh Populations in Donor-Matched Samples

Matched PBMC and MNC-T from adult donors were stained *ex vivo*.

(A) Dot plot illustrating the expression of CXCR5, PD-1, CXCR3, and ICOS within the total $CD4^+CD45RA^-$ cells in a representative matched blood and tonsil sample pair.

(B) Heatmaps showing the mean percentage of $CXCR3^+$ and $ICOS^+$ cells within populations expressing different combinations of CXCR5 and PD-1 in 12 donors. The white crossed boxes indicate the near-absence of the $PD\text{-}1^{hi}CXCR5^{hi}$ population in peripheral blood.

(C) Dot plot illustrating the gating strategy used to define populations of circulating $CXCR5^+PD\text{-}1^+$ Tfh (cTfh $CXCR3^+$, cTfh $CXCR3^-$) and $CXCR5^-$ non-Tfh memory cells (cNon-Tfh) and tonsillar $CXCR5^{hi}PD\text{-}1^{hi}$ GC Tfh (tTfh GC), $CXCR5^{int}PD\text{-}1^{int}$ (tTfh $CXCR3^+$, tTfh $CXCR3^-$) Tfh and $CXCR5^-PD\text{-}1^-$ non-Tfh memory cells (tNon-Tfh) within the total $CD4^+CD45RA^-$ T cell pool in one representative donor.

(D) The percentage of each Tfh/non-Tfh subset within the $CD4^+CD45RA^-$ memory T cell population in blood and tonsils from the 12 donors.

(E–G) Production of IL-21 (E), IL-4 (F), and IFN-γ (G) after PMA and ionomycin stimulation by Tfh and non-Tfh populations in 10 donors. Non-analogous subsets were compared within tonsil and peripheral blood using the Kruskal-Wallis test. $^*p < 0.05$, $^{**}p < 0.01$, $^{***}p < 0.001$, $^{****}p < 0.0001$. Boxes show means and quartiles, and whiskers show minima and maxima.

See also Figure S1.

2009; Yusuf et al., 2010). Production of IL-21 was lower in the other Tfh cell subsets and minimal in non-Tfh cells (Figure 1E). No significant differences in IL-4 production were observed between Tfh $CXCR3^+$, Tfh $CXCR3^-$, and non-Tfh cells from both tonsils and blood (Figure 1F). In line with the low expression of CXCR3 in Tfh GC cells, this population also exhibited minimal production of IFN-γ (Figure 1G), consistent with published data (Ma et al., 2009; Ploquin et al., 2011). In contrast, the major producers of IFN-γ were Tfh $CXCR3^+$ subsets from both tissues along with peripheral non-Tfh cells, which include canonical Th1 phenotype cells known to be the highest producers of anti-viral cytokines within $CD4^+$ cell subsets (Djuretic et al., 2007; Morita et al., 2011). Examples of cytokine staining for each cell subset are illustrated in Figures S1C–S1F.

Clonotypic Overlap between Peripheral and Tonsillar Tfh Cell Populations

To gain insight into the relationship between cTfh and tTfh populations, a TCR repertoire analysis was performed. The TCR clonotype sequence identifies clonal populations of T cells in different tissues. To compare the TCR repertoire of $CD4^+$ memory T cell populations, thawed PBMCs and MNC-Ts from 4 matched donors were stained, and tTfh GC, tTfh $CXCR3^+$, tTfh $CXCR3^-$, and tNon-Tfh cells from tonsils and cTfh $CXCR3^+$, cTfh $CXCR3^-$, and cNon-Tfh cells from blood were separated by fluorescence-activated cell sorting (FACS) (8,000–123,000 cells per subset). RNA was extracted, and 5′ (RACE) unique molecular identifiers (UMI)-controlled sequencing of the CDR3 region of the TCR Vβ chain repertoire was performed. Because fewer TCRs were sequenced from lower-frequency cell subsets, the frequency of each clonotype within its parent population was normalized, and subsequent analysis was performed on the most frequent 2,000 clonotypes (top2000) in each sample. This approach enabled insight to be gained into repertoire sharing between the most abundant clones in each of the analyzed populations.

The network analysis in Figure 2 illustrates the clonotypes shared between each population of blood $CD4^+$ T cells (cTfh $CXCR3^-$ [Figure 2A], cTfh $CXCR3^+$ [Figure 2C], and cNon-Tfh [Figure 2E]) and the different populations of tonsil (tTfh GC, tTfh $CXCR3^+$, tTfh $CXCR3^-$, and tNon-Tfh) cells without showing the connections between the tonsillar populations. The cTfh $CXCR3^-$ population showed the greatest clonotype sharing with tTfh GC; a total of 6.45% of clonotypes were found to be shared between these populations overall. This contrasts with findings from a recent study where no clonal overlap was observed between tTfh GC and the blood cTfh populations studied here (Hill et al., 2019), but it is consistent with another

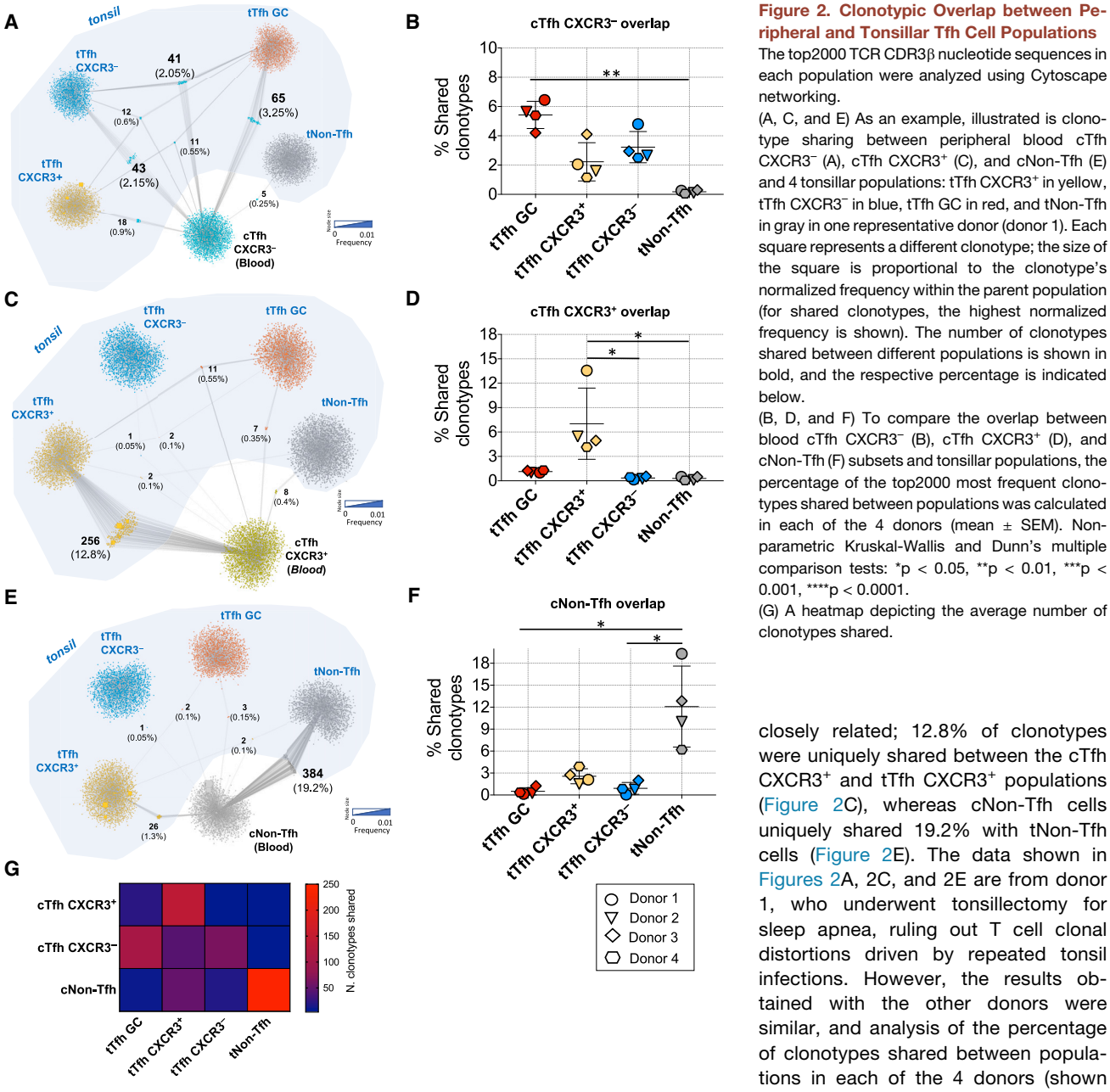

Figure 2. Clonotypic Overlap between Peripheral and Tonsillar Tfh Cell Populations

The top2000 TCR CDR3β nucleotide sequences in each population were analyzed using Cytoscape networking.

(A, C, and E) As an example, illustrated is clonotype sharing between peripheral blood cTfh CXCR3$^-$ (A), cTfh CXCR3$^+$ (C), and cNon-Tfh (E) and 4 tonsillar populations: tTfh CXCR3$^+$ in yellow, tTfh CXCR3$^-$ in blue, tTfh GC in red, and tNon-Tfh in gray in one representative donor (donor 1). Each square represents a different clonotype; the size of the square is proportional to the clonotype's normalized frequency within the parent population (for shared clonotypes, the highest normalized frequency is shown). The number of clonotypes shared between different populations is shown in bold, and the respective percentage is indicated below.

(B, D, and F) To compare the overlap between blood cTfh CXCR3$^-$ (B), cTfh CXCR3$^+$ (D), and cNon-Tfh (F) subsets and tonsillar populations, the percentage of the top2000 most frequent clonotypes shared between populations was calculated in each of the 4 donors (mean ± SEM). Non-parametric Kruskal-Wallis and Dunn's multiple comparison tests: *$p < 0.05$, **$p < 0.01$, ***$p < 0.001$, ****$p < 0.0001$.

(G) A heatmap depicting the average number of clonotypes shared.

recent report indicating that thoracic duct T cells with a CXCR5^{high} and PD-1^{high} phenotype show TCR sharing with cTfh (Vella et al., 2019). A total of 3.25% of clonotypes were uniquely shared between cTfh CXCR3$^-$ and tTfh GC, whereas others were also co-shared with the tTfh CXCR3$^-$ subset, with which cTfh CXCR3$^-$ also showed clonotype sharing; 2.05% of clonotypes were shared between all 3 of these populations, whereas a further 2.15% of clonotypes were uniquely shared between the cTfh CXCR3$^-$ and tTfh CXCR3$^-$ subsets (Figure 2A). In contrast, cTfh CXCR3$^+$ and cNon-Tfh populations each showed extensive repertoire overlap only with the tonsil CD4$^+$ population to which they were phenotypically most closely related; 12.8% of clonotypes were uniquely shared between the cTfh CXCR3$^+$ and tTfh CXCR3$^+$ populations (Figure 2C), whereas cNon-Tfh cells uniquely shared 19.2% with tNon-Tfh cells (Figure 2E). The data shown in Figures 2A, 2C, and 2E are from donor 1, who underwent tonsillectomy for sleep apnea, ruling out T cell clonal distortions driven by repeated tonsil infections. However, the results obtained with the other donors were similar, and analysis of the percentage of clonotypes shared between populations in each of the 4 donors (shown in Figures 2B, 2D, and 2F) confirms the overlap between cTfh CXCR3$^-$ and both tTfh GC and tTfh CXCR3$^-$ populations (Figure 2B) and the extensive clonotype sharing of cTfh CXCR3$^+$ with tTfh CXCR3$^+$ cells (Figure 2D) and of cNon-Tfh with tNon-Tfh cells (Figure 2F). The heatmap (Figure 2G) displays the number of clonotypes shared between populations for all 4 donors.

For a deeper TCR repertoire comparison, it was important to also consider the size of each clonotype (weighted analysis) to gauge the repertoire overlap in terms of cell numbers. For each tonsil and blood comparison, the normalized F2 metric of VDJtools (Shugay et al., 2013) was calculated. The F2 is the sum of the geometric means between the frequencies of shared clonotypes, the greater the F2 value between two subsets, the

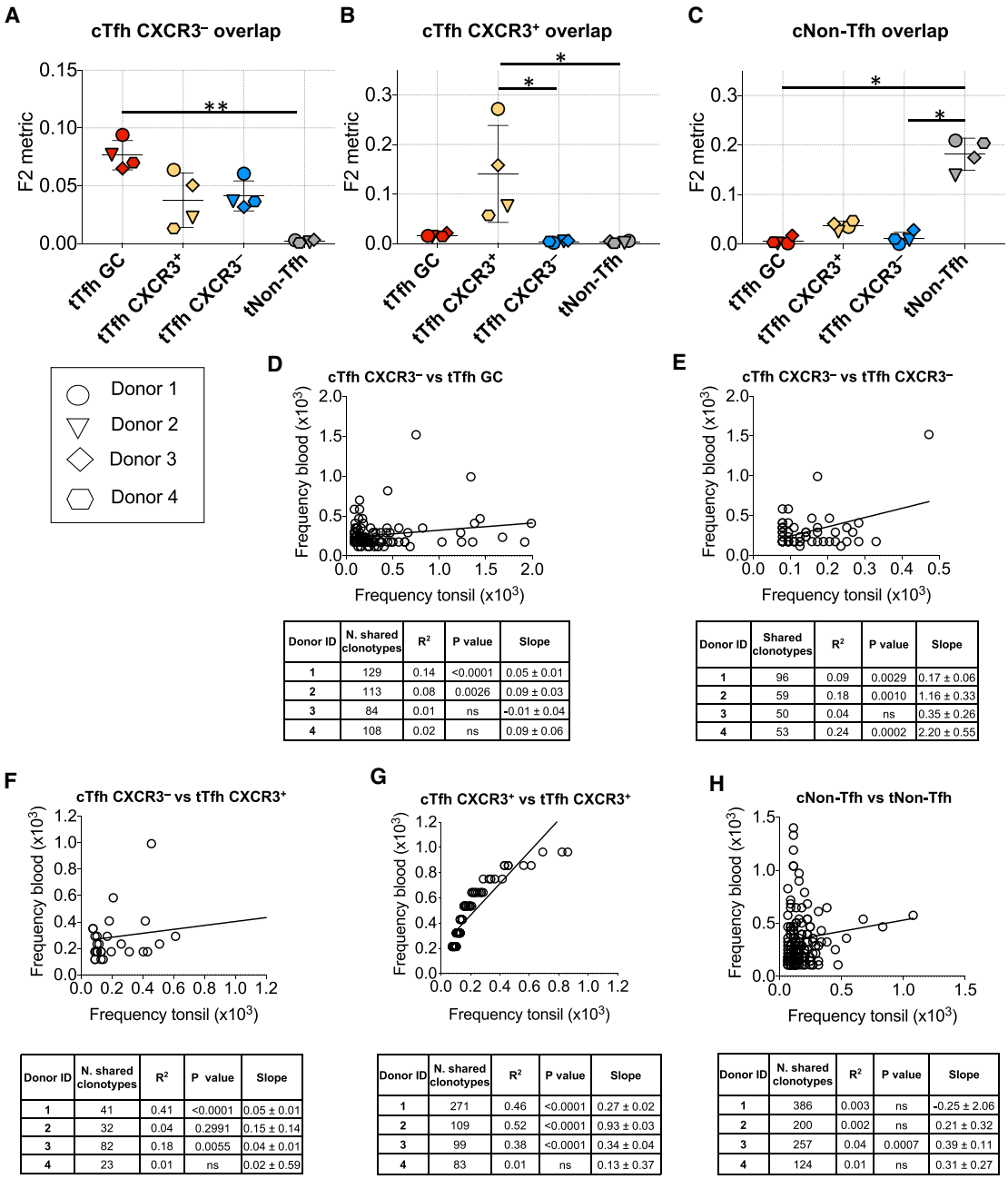

Donor ID	N. shared clonotypes	R^2	P value	Slope
1	129	0.14	<0.0001	0.05 ± 0.01
2	113	0.08	0.0026	0.09 ± 0.03
3	84	0.01	ns	-0.01 ± 0.04
4	108	0.02	ns	0.09 ± 0.06

Donor ID	Shared clonotypes	R^2	P value	Slope
1	96	0.09	0.0029	0.17 ± 0.06
2	59	0.18	0.0010	1.16 ± 0.33
3	50	0.04	ns	0.35 ± 0.26
4	53	0.24	0.0002	2.20 ± 0.55

Donor ID	N. shared clonotypes	R^2	P value	Slope
1	41	0.41	<0.0001	0.05 ± 0.01
2	32	0.04	0.2991	0.15 ± 0.14
3	82	0.18	0.0055	0.04 ± 0.01
4	23	0.01	ns	0.02 ± 0.59

Donor ID	N. shared clonotypes	R^2	P value	Slope
1	271	0.46	<0.0001	0.27 ± 0.02
2	109	0.52	<0.0001	0.93 ± 0.03
3	99	0.38	<0.0001	0.34 ± 0.04
4	83	0.01	ns	0.13 ± 0.37

Donor ID	N. shared clonotypes	R^2	P value	Slope
1	386	0.003	ns	-0.25 ± 2.06
2	200	0.002	ns	0.21 ± 0.32
3	257	0.04	0.0007	0.39 ± 0.11
4	124	0.01	ns	0.31 ± 0.27

Figure 3. Size Similarities in Clonotypes Shared between cTfh and tTfh

(A–C) Overlap between TCR CDR3β nucleotide sequences of the top2000 most frequent clonotypes of blood cTfh CXCR3$^-$ (A), cTfh CXCR3$^+$ (B), and cNon-Tfh (C) populations with each tonsil population, as represented by the normalized F2 metric (mean ± SEM). Non-parametric Kruskal-Wallis and Dunn's multiple comparison test: *$p < 0.05$, **$p < 0.01$, ***$p < 0.001$, ****$p < 0.0001$.

(D–H) Linear regression analysis of the correlation between the within-population frequency of the shared clonotypes in the two parent populations where clonotype sharing between populations was observed: cTfh CXCR3$^-$ with tTfh GC (D), tTfh CXCR3$^-$ with cTfh CXCR3$^-$ (E), cTfh CXCR3$^-$ with tTfh CXCR3$^+$ (F), cTfh CXCR3$^+$ with tTfh CXCR3$^+$ (G), and cNon-Tfh with tNon-Tfh (H). Each graph illustrates a representative donor, and the tables show the number of shared clonotypes, the square of the Pearson correlation coefficient (R^2), the slope value for each donor, and the p value of the significance of the difference in the slope from zero (ns, not significant).

higher the number of T cells bearing the shared TCR variants (Izraelson et al., 2018). This analysis confirmed the repertoire similarity of cTfh CXCR3$^-$ with tTfh GC and tTfh CXCR3$^-$ populations and identified a connection between cTfh CXCR3$^-$ and tTfh CXCR3$^+$ cells (Figure 3A). Likewise, the F2 metric also validated the overlap of cTfh CXCR3$^+$ with tTfh CXCR3$^+$ cells (Figure 3B)

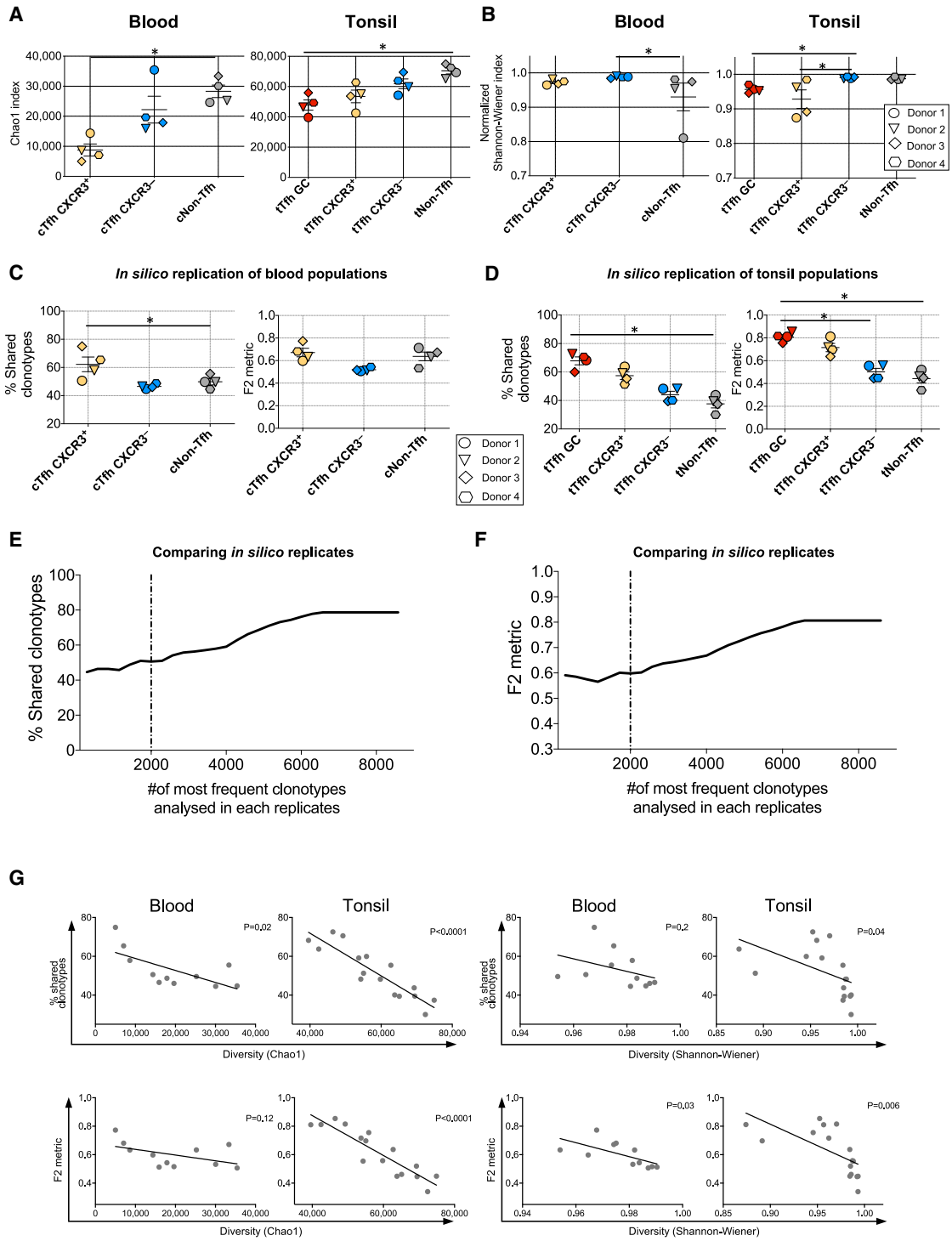

Figure 4. Repertoire Diversity Correlates with the Degree of Clonotypic Overlap from the *In Silico* Resampling Analysis

(A and B) Chao1 index (A) and normalized Shannon-Wiener index (B) of the top2000 frequencies for each population of cells analyzed in blood and tonsils from the 4 donors (mean ± SEM). Clonotypes of each subset were resampled using the bootstrap method.

(C and D) The percentage of the top2000 shared clonotypes and the normalized F2 metric (mean ± SEM) of the overlap between the two replicates of blood (C) cTfh CXCR3$^+$, cTfh CXCR3$^-$, and cNon-Tfh as well as tonsil (D) tTfh GC, tTfh CXCR3$^+$, tTfh CXCR3$^-$, and tNon-Tfh populations is shown for all 4 donors (mean ± SEM). Non-parametric Kruskal-Wallis and Dunn's multiple comparison test: *$p < 0.05$, **$p < 0.01$, ***$p < 0.001$, ****$p < 0.0001$.

(legend continued on next page)

and the extensive overlap of cNon-Tfh with tNon-Tfh cells and identified weaker connections with tTfh populations (Figure 3C).

To better visualize the similarity between these two compartments, where clonotype sharing was observed, the frequencies of each shared clonotype were analyzed by linear regression. Although there was consistent overlap between cTfh CXCR3$^-$ and tTfh GC cells (Figure 3D), comparison of the relative sizes of clonotypes shared by the two different compartments was significant in only 2 of the 4 donors, with a low Pearson correlation coefficient (R^2; 0.08 and 0.14). In all cases, the slope of the correlation was less than 1, indicating that, in tonsils, most of the clonotypes are more expanded than in the blood. A similar scenario was observed for cTfh CXCR3$^-$ versus tTfh CXCR3$^-$ subsets (Figure 3E) and cTfh CXCR3$^-$ versus tTfh CXCR3$^+$ populations (Figure 3F). The correspondence between cTfh CXCR3$^+$ and tTfh CXCR3$^+$ populations remained the strongest; the sizes of the clonotypes shared between these populations were also very similar, significant ($p < 0.0001$) in 3 of the 4 donors (Figure 3G). For the cNon-Tfh and tNon-Tfh comparison, despite the high number of clonotypes shared (124–386), the size of the clonotypes was very different between blood and tonsils, making the linear correlation significant in only 1 of the 4 donors (Figure 3H).

Repertoire Diversity Correlates with the Degree of Clonotypic Overlap from the *In Silico* Resampling Analysis

To compare the repertoire diversity of each population, the nonparametric Chao1 index (Figure 4A) was calculated to estimate the richness of the number of unobserved elements in the set considered (Colwell et al., 2012; Eren et al., 2012). The normalized Shannon-Wiener index was also calculated to measure the entropy of each TCR sequence population (Figure 4B) based on the uncertainty of predicting the next sequence in a string. The two parameters describe the repertoire diversity from different perspectives; Chao1 is based on relative distributions of low-frequency clonotypes, whereas Shannon-Wiener takes into account large clonal expansions (Izraelson et al., 2018). Notably, an increase of diversity was observed in blood from cTfh CXCR3$^+$ to cTfh CXCR3$^-$ and cNon-Tfh cells; likewise, in tonsils, tTfh GC cells were less diverse than tNon-Tfh subsets, which showed the highest value of both Chao1 and normalized Shannon-Wiener index values.

To improve our understanding of the magnitude of the overlap observed between CD4$^+$ T cell subsets in blood and tonsils, which was based on analysis of a limited number of cells from each population, an *in silico* replication using the bootstrap method was applied to re-sample the clonotypes in each subset. When re-sampling the same subset twice, populations from the blood (Figures 4C and S2A) showed, on average, an overlap between sampling 1 and sampling 2 of 50%, with cTfh CXCR3$^+$ cells slightly higher (60%–70%). In tonsil populations (Figures 4D and S2A), the highest reproducibility was reported for tTfh GC cells, with decreasing levels of overlap observed for tTfh CXCR3$^+$ and tTfh CXCR3$^-$ populations and the lowest with tNon-Tfh cells. A similar trend was reported from the weighted analysis represented by the F2 metric analysis.

When increasing the number of clonotypes considered, the prediction did not reach complete overlap but, rather, a plateau of 60% of unweighted (Figure 4E) and 0.8 weighted (Figure 4F) analysis, respectively. As expected, the degree of overlap was inversely related to population diversity (Figure 4G) and was more pronounced for tonsils compared with blood, confirming that, when a population is less diverse, the degree of overlap on *in silico* resampling is higher. The overlap of the same population was also assessed experimentally in non-Tfh (Figure S2B) and Tfh cells (Figure S2C) from 3 additional donors and was found to be less than 30% for non-Tfh and less than 52% for Tfh subsets.

These results show that, even when re-sampling exactly the same set of sequences or sequencing two vials of the same sorted population, the repertoire overlap is never complete (100% and F2 = 1), and it changes depending on the diversity of the subset considered and the size of the sample (Shugay et al., 2013). This implies that the degree of overlap observed experimentally is an underestimate, reflecting the relatively small sample size and reinforcing the conclusion that there is substantial repertoire overlap between blood and tonsil Tfh populations.

Tfh Cell Subsets Are Clonotypically Distinct from Non-Tfh Cells

Whether Tfh cells make up a distinct population of CD4$^+$ T cells with a unique program of differentiation or are a subset of the memory CD4$^+$ T cell compartment in a transient activation state is still debated (Baumjohann et al., 2013; Crotty, 2014; Herati et al., 2017; Vinuesa et al., 2005; Weber et al., 2015).

A cytoscape networking analysis revealed only a very low level of TCR Vβ repertoire overlap between cTfh CXCR3$^+$, cTfh CXCR3$^-$, and cNon-Tfh populations in the blood compartment (Figure 5A). This was true for both comparisons of cTfh CXCR3$^+$ versus cTfh CXCR3$^-$ (0.8%) and cTfh subsets versus cNon-Tfh (0.3%–1%) populations. In addition, very few clonotypes were shared between all 3 populations (0.2%). These results were consistent across all 4 donors analyzed (Figure S3). Similarly, tTfh cells (either CXCR3$^+$, CXCR3$^-$, or GC) were also notably distinct from the tNon-Tfh population (Figure 5B), with very little repertoire overlap (0.1%–0.3%). In contrast, the 3 tTfh populations showed considerable overlap with each other: tTfh CXCR3$^+$ with tTfh CXCR3$^-$ and Tfh GC (0.8%–3.1%), tTfh CXCR3$^+$ with tTfh GC (3.6%–7.4%), tTfh CXCR3$^-$ with tTfh GC (4%–14.9%), and tTfh CXCR3$^+$ with tTfh CXCR3$^-$ (2.7%–6.3%) (Figure 5C). Although the extent of the repertoire overlap between the tTfh populations was variable in different donors, clonotype sharing between the 3 tTfh cell populations was observed in all 4 donors, especially between the tTfh CXCR3$^-$ and tTfh GC subsets. A normalized F2 metric analysis confirmed the overlap between tTfh CXCR3$^-$ and

(E and F) Unweighted (E) and weighted (F) analysis of the replicate overlap at increasing numbers of clonotypes considered from a representative population (cTfh CXCR3$^+$ from donor 1).

(G) The graphs show the linear regression correlation between the repertoire overlap, expressed either as percentage of shared clonotypes or normalized F2 metric, with both diversity indexes (Chao1 and normalized Shannon-Wiener) in all blood and tonsil populations from the 4 donors analyzed.

See also Figure S2.

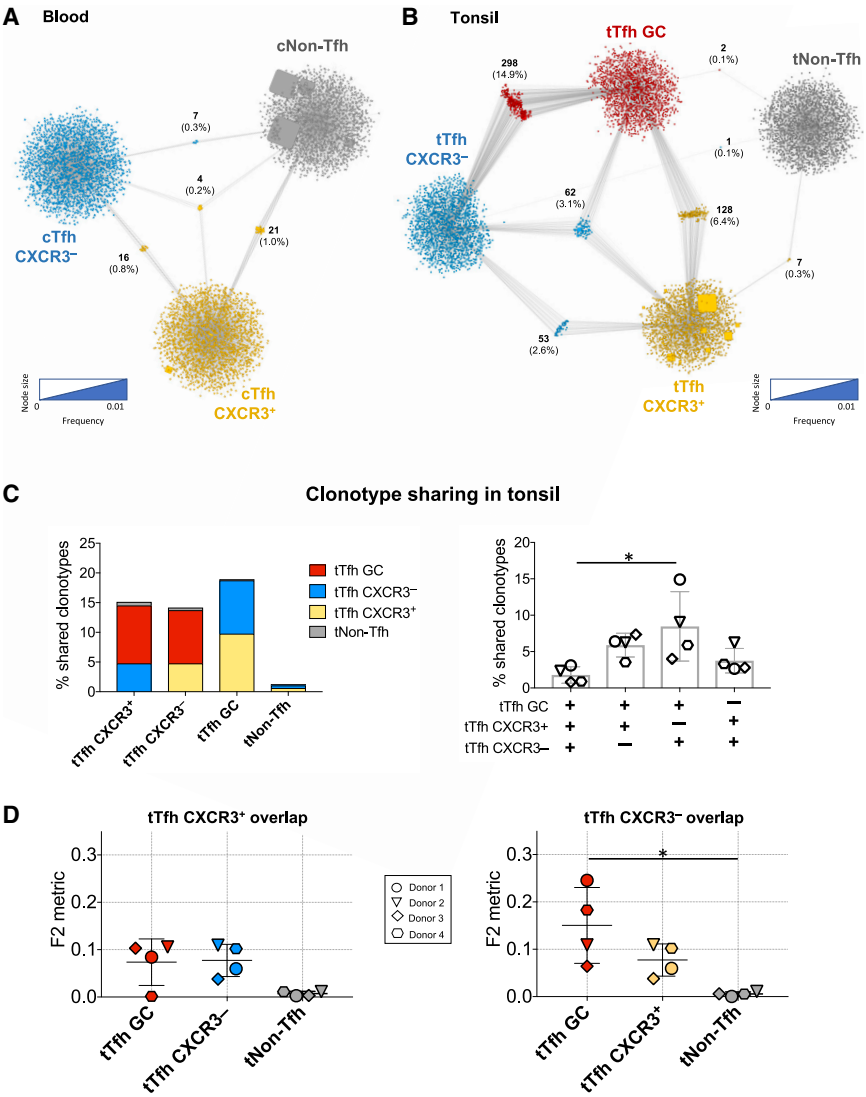

Figure 5. Tfh Cell Subsets Are Clonotypically Distinct from Non-Tfh Cells

The top2000 TCR Vβ CDR3 nucleotide sequences of each population were analyzed by Cytoscape networking.

(A and B) Examples of (A) clonotype sharing between peripheral blood cTfh CXCR3$^+$ (yellow), cTfh CXCR3$^-$ (blue), and cNon-Tfh (gray) populations and (B) clonotype sharing between tonsillar populations tTfh CXCR3$^+$ (yellow), tTfh CXCR3$^-$ (blue), tTfh GC (red), and tNon-Tfh (gray) populations in one representative donor (donor 1). Results are expressed as in Figure 2.

(C) The percentage of the top2000 total shared clonotypes in addition to the uniquely shared clonotypes between tonsil populations was calculated in each of the 4 donors (mean ± SEM).

(D) The normalized F2 metric of the top2000 frequencies was also calculated for the overlap between tTfh CXCR3$^+$ and tTfh CXCR3$^-$ subsets and each of the other populations analyzed in the 4 donors (mean ± SEM). Non-parametric Kruskal-Wallis and Dunn's multiple comparison test: *p < 0.05, **p < 0.01, ***p < 0.001, ****p < 0.0001.

(E) The table shows the number of shared clonotypes, the square of R^2 in their size within populations, the slope value, and the p value of the difference in the slope from zero.

See also Figure S3.

E

Tonsil	tTfh CXCR3+ vs tTfh CXCR3–				tTfh CXCR3+ vs tTfh GC				tTfh CXCR3– vs tTfh GC			
Donor ID	Shared clonotypes	R^2	P value	Slope	Shared clonotypes	R^2	P value	Slope	Shared clonotypes	R^2	P value	Slope
1	115	0.35	<0.0001	0.77	190	0.03	0.01	0.37	360	0.33	<0.0001	2.55
2	172	0.04	0.007	0.10	214	0.01	*ns*	0.06	229	0.01	*ns*	*0.23*
3	70	0.08	0.01	0.18	161	0.01	*ns*	0.06	96	0.03	*ns*	1.11
4	84	0.01	*ns*	-0.01	89	0.03	*ns*	0.31	136	0.01	*ns*	-0.04

tTfh GC subsets and the repertoire distance between all tTfh populations and tNon-Tfh (Figure 5D). Despite the numerous clonotypes shared between tTfh CXCR3$^+$ and tTfh CXCR3$^-$ (70–172), tTfh CXCR3$^+$ and tTfh GC (89–214), and tTfh CXCR3$^-$ and tTfh GC (96–360), the relative immunodominance of the shared clonotypes differed substantially; the correlations were $R^2 < 0.36$ and, in the majority of cases, not significant (Figure 5E).

Influenza Virus HA-Specific Clones Are Predominantly Found in cTfh CXCR3$^+$ and cNon-Tfh Populations

To compare the repertoire of antigen-specific Tfh and non-Tfh cells in peripheral blood and their representation in tonsil populations, responses to the HA protein H3 from influenza virus A/Wisconsin/67/2005 were studied (Alam and Sant, 2011; Fazilleau et al., 2007; Sant et al., 2018). To assess the relative abundance of memory CD4$^+$ T cells reactive with HA protein, the T cell library method (Geiger et al., 2009) was used to determine the precursor frequency of HA-reactive cells in isolated memory CD4$^+$ T cell populations and to characterize the cTfh and cNon-Tfh CD4$^+$ memory repertoire in 3 healthy donors, samples from whom were obtained from the National Health Service (NHS) Blood Transfusion Service (Figure 6A). All 3 donors showed enrichment of HA-specific T cells in the cTfh CXCR3$^+$ and cNon-Tfh populations. Few responding HA-specific cTfh CXCR3$^-$ cells were found, and they were only detected in donor A. The precursor frequency of antigen-specific cells per million was calculated within each subset (Figure 6B). Donors A and B showed the highest HA-specific precursor frequency in both cTfh CXCR3$^+$ and cNon-Tfh populations (530–550 and 280–150 antigen-specific cells/million). The differences observed in the 3 donors analyzed likely reflects the diverse prior antigenic exposure of each individual.

Having shown that HA-specific cTfh cells were present in peripheral blood, the antigen-specific cTfh repertoires of 4 further donors, from whom tonsil samples were available in addition to peripheral blood samples (donors 1, 2, 3, and 4), were compared

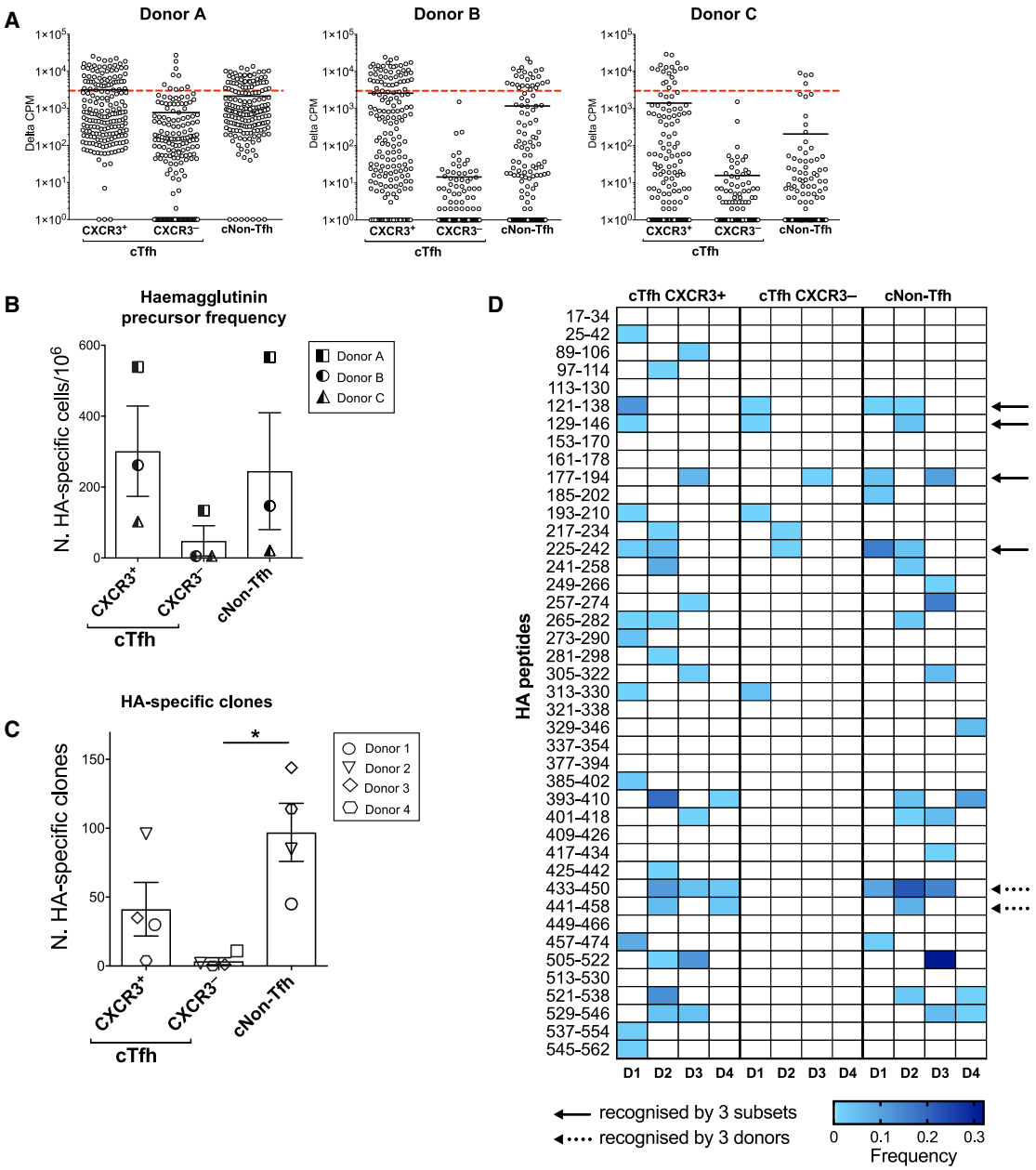

Figure 6. Influenza Virus HA-Specific Clones Are Predominantly Found in cTfh CXCR3$^+$ and cNon-Tfh Populations

(A) T cell libraries generated from Tfh and non-Tfh subsets sorted from three healthy blood donors from the National Health Service (NHS) Blood Transfusion Service were tested against the influenza H3/Wisconsin HA protein. The proliferation of each individual cell line (increase in counts above background, delta cpm) is shown (mean ± SEM). The red dotted line represents the cutoff used for identification of a positive response (defined as >3000 cpm, with a stimulation index >5).

(B) Calculated precursor frequency of HA-specific cells per 10^6 cells in each subset (mean ± SEM).

(C) Bar graph showing the number of influenza H1/California HA-specific T cell clones generated from each cell subset in the 4 further donors from whom matched tonsil samples were available. Non-parametric Kruskal-Wallis and Dunn's multiple comparison test: *$p < 0.05$, **$p < 0.01$, ***$p < 0.001$, ****$p < 0.0001$.

(D) Epitopes recognized by HA-specific cTfh CXCR3$^+$, cTfh CXCR3$^-$, and cNon-Tfh clones were mapped, and the frequency of clones recognizing each peptide, normalized to the total frequency of HA-specific clones in all donors (D1, D2, D3, and D4), is plotted in the heatmap. The solid arrows highlight the peptides recognized by 3 subsets and the dashed arrows the peptides recognized by 3 donors.

See also Figure S4.

with the entire repertoire of T cells in tonsillar cell subsets from the same individual. To confirm influenza virus exposure, plasma samples from the 4 donors were screened for the presence of HA-specific antibodies, evaluating immunoglobulin G (IgG) reactivity with HA protein from influenza virus strain A/California/07/2009, H1N1 (Figure S4A) and IgG reactivity with trivalent (H1,

A

Clones specific for peptide 225-242: KKFKPEIAIRPKVRDQEG

DONOR ID	CLONE TYPE	CLONE ID	TRAV	AA α CDR3	TRAJ	TRBV	AA β CDR3	TRBJ
Donor 1	cTfh CXCR3+	5	26-1	CIVRVAGGSYIPT	6	4-2	CASSQDYGLNYNEQF	2-1
Donor 1	cTfh CXCR3+	13	39	CAVLPVSRNTGKLI	37	10-1	CASSEPGVGSSYNEQF	2-1
Donor 1	cNon-Tfh	6	8-4	CAVTFGGFKTI	9	24-1	CATSDNGLGQTYNEQF	2-1
Donor 1	cNon-Tfh	7	39	CAVVLQGGEKLV	57	6-5	CASSSRGPGRYSNQPQH	1-5
Donor 1	cNon-Tfh	26	10	CVVSGGSNYKLT	53	24-1	CATSDSGLAGGGLSELF	2-2
Donor 2	cTfh CXCR3+	49	23/DV6	CAASARETGANNLF	36	15	CATSRDRVGEKLF	1-4
Donor 2	cTfh CXCR3+	69	26-2	CILPRNYGGSQGNLI	42	6-5	CASSNQGTQY	2-5
			35	CAGPLRSNDYKLS	20			
Donor 2	cTfh CXCR3–	1	23/DV6	CAASMRGEYGQNFV	26	6-5	CASSYSWGITEAF	1-1
Donor 2	cNon-Tfh	41	39	CAVVLEGTGTASKLT	44	5-1	CASSLWGSGSAPYEQY	2-7
Donor 2	cNon-Tfh	42	23/DV6	CAASSRGSQGNLI	42	24-1	CATSDEAGGSDEQF	2-1

Clones specific for peptide 177-194: KLSKSYINDKGKEVLVLW

DONOR ID	CLONE TYPE	CLONE ID	TRAV	AA α CDR3	TRAJ	TRBV	AA β CDR3	TRBJ
Donor 3	cTfh CXCR3+	1	35	CAGDRDDKII	30	2	CASRSGAYNEQF	2-1
Donor 3	cTfh CXCR3+	18	35	CAGDRDDKII	30	2	CASRSGAYNEQF	2-1
Donor 3	cTfh CXCR3+	19	35	CAGDRDDKII	30	2	CASRSGAYNEQF	2-1
Donor 3	cTfh CXCR3+	24	35	CAGDRDDKII	30	2	CASRSGAYNEQF	2-1
Donor 3	cTfh CXCR3+	31	35	CAGDRDDKII	30	2	CASRSGAYNEQF	2-1
Donor 3	cTfh CXCR3–	1	9-2	CALFDTGRRALT	5	2	CASSWGQGKVRNQPQH	1-5
Donor 3	cNon-Tfh	22	22	CAVEGAGGSYIPT	6	9	CASSVGVGTNNEKLF	1-4

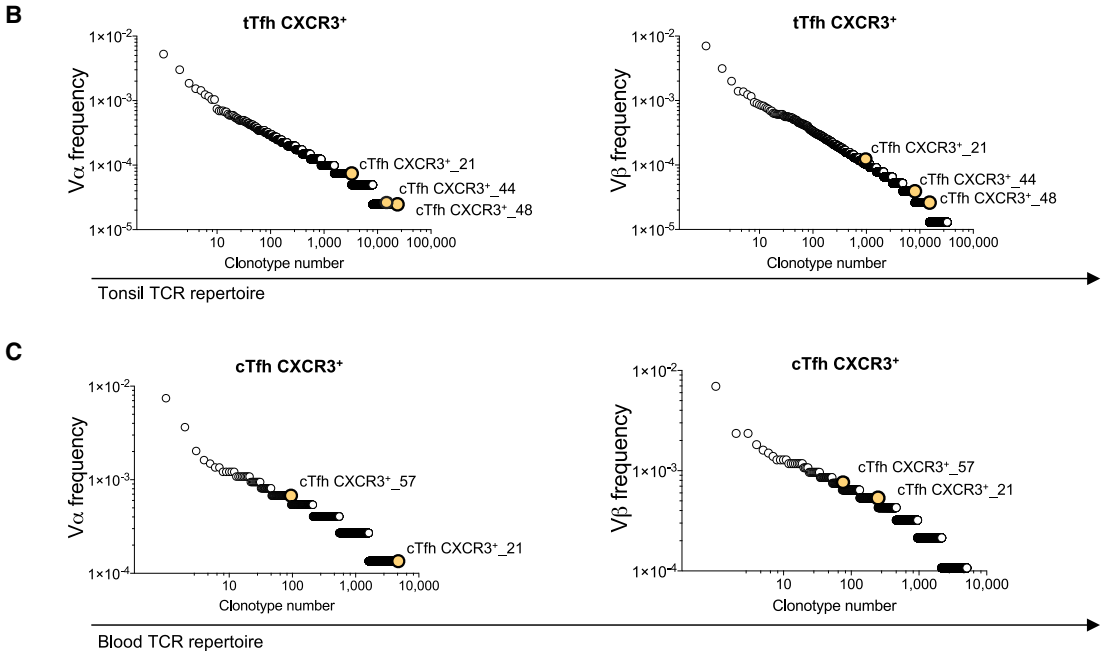

Figure 7. HA-Specific cTfh and cNon-Tfh Clones Do Not Overlap, and HA-Specific cTfh CXCR3⁺ T Cell Clonotypes Can Be Detected in the tTfh CXCR3⁺ Subset

(A) TCR CDR3α and CDR3β sequencing was performed on clones specific for the same HA H1/California peptide that had been generated from either the cTfh CXCR3⁺, cTfh CXCR3⁻, or cNon-Tfh subset in 3 donors. For each clone, the peptide specificity, the CDR3α and CDR3β amino acid (AA) sequences, and *TRAV/TRAJ* and *TRBV/TRBJ* gene usage are shown. Clones are grouped based on the peptide recognized.

(legend continued on next page)

H3, and B) influenza vaccine 2017 (TIV) (Figure S4B) by ELISA. IgG antibodies reactive with both HA protein and TIV were detected in all 4 donors. Tfh cell clones specific for HA protein (H1) were then generated from peripheral blood cTfh CXCR3$^+$, cTfh CXCR3$^-$, and cNon-Tfh populations of each donor. As shown in Figure 6C, the highest numbers of HA-specific clones were derived from either cTfh CXCR3$^+$ or cNon-Tfh populations. These were the subsets in which antigen-specific cloning efficiency was greatest (Figure S4D). Based on the percentage of activated ICOS$^+$CD25$^+$ cells after 7 days of stimulation (Figure S4C) and the proportion of the clones generated from the activated populations that were subsequently confirmed to be HA-reactive by proliferation, it was possible to gain estimates of the number of HA-specific cells within each subset (Figure S4E) or within the CD4$^+$ memory compartment (Figure S4F). The data confirmed that HA-specific T cells were enriched in the cTfh CXCR3$^+$ and cNon-Tfh populations, whereas, as expected, only a few HA-specific cells were found in the cTfh CXCR3$^-$ compartment (Bentebibel et al., 2013; Pallikkuth et al., 2012).

The epitopes recognized by HA-specific T cell clones were then mapped using a matrix of overlapping peptides from HA/California (H1). The data from cTfh CXCR3$^+$ and cNon-Tfh clones highlighted the breadth of HA epitopes recognized in each donor and suggested a difference in the pattern of epitopes recognized by cTfh and cNon-Tfh subsets because only a few peptides per donor were recognized by all three types of cells (Figure 6D, solid arrows). Epitopes recognized by at least 3 donors are highlighted in Figure 6D with dashed arrows; peptide 433–450 was the most universally targeted, being recognized by cTfh CXCR3$^+$ clones from donors 2, 3, and 4 and by cNon-Tfh clones from donors 1, 2, and 3. The number of cTfh CXCR3$^-$ clones was low, and none of the clones recognized epitopes targeted in at least 3 donors, including peptides 433–450 and 441–458.

HA-Specific cTfh CXCR3$^+$ T Cell Clonotypes Can Be Detected in the tTfh CXCR3$^+$ Subset

To determine whether clones with the same peptide specificity also express the same TCR, the CDR3α and CDR3β gene transcripts of a subset of HA-specific clones from donors 1, 2, and 3 were sequenced (Figure 7A). These data showed that, when cTfh CXCR3$^+$, cTfh CXCR3$^-$, and cNon-Tfh cell clones were specific for the same peptide (for example, peptide 225–242 for donors 1 and 2 and peptide 177–194 for donor 3), they did not share the same CDR3 region and were therefore clonotypically distinct. In some cases, even when 2 clones were specific for the same peptide and belonged to two different lineages, they used TCRα or TCRβ chains from the same family. For instance, in donor 2, clones 49 (cTfh CXCR3$^+$), 1 (cTfh CXCR3$^-$), and 42 (cNon-Tfh) specific for peptide 225–242 exhibited different CDR3α sequences, but all three TCRα chains belonged to the same TRAV23/DV6 family. Also, in donor 3, clones 1 (cTfh CXCR3$^+$) and 1 (cTfh- CXCR3$^-$) specific for peptide 177–194, which again had different CDR3α sequences, possessed TCRβ chains belonging to the same family (TRBV2). Additional sequences from donor 1 are shown in Figure S5A.

We next investigated whether the TCRα or TCRβ chain sequences identified in HA-specific T cell clones were detectable in the overall repertoire of CD4$^+$ T cell subsets from both tonsils and peripheral blood, which had been evaluated by non-paired sequencing of αβ TCRs. Because both the TCRα and TCRβ chain of each HA-specific T cell clone were available, it was possible to determine the presence or absence of each clonotype on the basis of detection of both chains in the subsets analyzed. Although only 75 HA-specific clones were sequenced, 3 cTfh CXCR3$^+$ clones from donor 2 were found in the tTfh CXCR3$^+$ repertoire from the same donor (Figure 7B), and two clones, also from donor 2, were detected in the cTfh CXCR3$^+$ subset (Figure 7C). The tables show the frequency of the clonotype of interest observed in tonsils (Figure S5B) and in blood (Figure S5C) for both TCR chains. The presence of HA-specific Tfh clones initially derived from PBMCs in the tTfh CXCR3$^+$ repertoire of the same donor confirmed the direct relationship between antigen-specific circulating and tTfh cells.

DISCUSSION

This work analyses the clonotypic overlap of Tfh cell subsets from peripheral blood and tonsillar cell populations. Repertoire sharing was selectively detected between blood and tonsillar populations with similar phenotypic characteristics, defined as cTfh CXCR3$^+$ and tTfh CXCR3$^+$, cTfh CXCR3$^-$ and tTfh GC/tTfh CXCR3$^-$, and cNon-Tfh and tNon-Tfh subsets. These results suggest that, in a steady-state condition, the clonal composition of the CXCR5$^+$PD-1$^+$ circulating cTfh population reflects that of tonsil-resident tTfh cells. The TCR repertoire analysis also provided evidence of a clear distinction between Tfh and non-Tfh cell populations. These observations were confirmed by a parallel analysis of antigen-specific T cell clones recognizing HA from influenza virus. Therefore, separation of Tfh cells from the total memory CD4$^+$ T cell pool is necessary to investigate the specificity of the follicular T cell response.

In line with previous observations, Tfh GC cells (CXCR5^{hi}PD-1^{hi}) were the major sources of IL-21 and IL-4 and were only present in tonsils (Dan et al., 2019; He et al., 2013; Heit et al., 2017; Locci et al., 2013). The presence of effector Tfh GC cells in tonsils suggested a probable ongoing immune response in this tissue (Baumjohann et al., 2013; Hansen et al., 2017; Havenar-Daughton et al., 2016), which was likely driven by residual antigen from prior infections because antigen can persist for months or years on follicular dendritic cells in draining lymph nodes (Tew and Mandel, 1979; Tew et al., 1984), We showed that Tfh GC cells

(B and C) The TCR CDR3α and CDR3β region sequences of 75 HA-specific clones generated from the blood populations were determined, and the *ex vivo* Vα and Vβ repertoires of tonsil and blood Tfh and non-Tfh populations from the same subject were searched for matching sequences. Matches were detected only in donor 2. The frequency distributions of each of the individual clonotypes detected in the tonsil tTfh CXCR3$^+$ (B) and peripheral blood cTfh CXCR3$^+$ (C) repertoires are shown, with yellow circles indicating the sequences that matched those of the HA-specific cTfh CXCR3$^+$ clones generated from the peripheral blood of the same donor.
See also Figure S5.

are enriched in CXCR3$^-$ cells and produced little IFN-γ (Ma et al., 2009; Ploquin et al., 2011). The lack of CXCR3 expression by Tfh GC cells is consistent with their specific effector function inside the GC, where they do not need to directly face inflammation but actively participate in formation of neutralizing antibodies (Djuretic et al., 2007; He et al., 2013). Phenotypic features highlighted similarities, in particular between tTfh CXCR3$^+$ and cTfh CXCR3$^+$ subsets, but also heterogeneity between blood and tonsil populations (Chevalier et al., 2011; He et al., 2013). These differences may be driven by stimuli present in the respective local environments (Wong et al., 2016) and reflect selective recruitment, retention, or differentiation of populations at particular sites (Durand et al., 2019).

To better determine the relationship between circulating and tTfh cell populations, we explored TCR repertoires, given that a cell's TCR does not change with cellular location or differentiation. The vast TCR diversity within each individual (estimated at 10^8) and the number of cells sequenced per sample (10^3–10^5) always constrains TCR repertoire studies and poses caveats requiring the use of technical or *in silico* replicates to confirm the primary observations. However, TCR deep sequencing highlighted correlations between tonsil and blood Tfh and non-Tfh populations. Although RNA-based TCR sequencing provides relatively good repertoire coverage, it is not possible to calculate the absolute frequency of each clonotype with the analyzed populations (Heather et al., 2018; Rosati et al., 2017). However, we combined both weighted (the F2 metric) and unweighted (percentage of shared clonotypes) analyses and observed similar trends, validating the repertoire overlap observed between populations.

Effector Tfh GC cells from tonsils and tTfh CXCR3$^-$ cells showed a moderate repertoire overlap with cTfh CXCR3$^-$ cells from peripheral blood. Although a Tfh GC/cTfh CXCR3$^-$ relationship between tonsils and blood has been demonstrated previously in terms of gene expression (Locci et al., 2013), our analysis of donor-matched tissues directly demonstrates that the same Tfh clones are present in both tonsils and the blood CXCR5$^+$PD-1$^+$ cTfh compartment. The relatively modest overlap might be explained by the specific and localized role of Tfh GC cells during their effector phase in the GC (Groom and Luster, 2011). Consistent with this, we observed that shared clonotypes are more expanded in tonsils than in blood, suggesting selective retention of a locally expanded Tfh population. The clonotype sharing between tTfh GC and tTfh CXCR3$^-$ cells may reflect the fact that both are enriched for cells recognizing locally presented antigens, with Tfh GC potentially originating from or sharing common precursors with Tfh CXCR3$^-$ (Crotty, 2018; Locci et al., 2013). In contrast, the cTfh CXCR3$^-$ population probably has a much more promiscuous origin because it is likely to contain antigen-experienced Tfh cells that have exited from lymphoid tissues before or after becoming effector Tfh GC cells during both the ongoing and prior immune responses. It is also possible that cTfh cells are recruited from the periphery in response to local chronic infection in the tonsils.

This study does not address the differentiation and generation of Tfh CXCR3$^+$ cells, but the convergence in clonotypic repertoire observed between peripheral blood and tonsils was striking. This suggests high mobility of these types of cells from secondary lymphoid organs to the peripheral circulation or vice versa. The minor but consistent repertoire sharing between Tfh CXCR3$^+$ and Tfh CXCR3$^-$ cells in tonsils may result from tTfh cell differentiation from one phenotype to the other or plasticity among CXCR3$^+$ and CXCR3$^-$ phenotypes, observed previously in canonical T helper subsets (Becattini et al., 2014; Hegazy et al., 2010).

The repertoire sharing observed between non-Tfh cells in tonsils and blood confirms communication between the two tissues and suggests that, after priming, CD4$^+$ T cells from secondary lymphoid organs may exit into the peripheral circulation to pursue their effector function but also that circulating non-Tfh cells may be recruited to the tonsils to react to ongoing chronic infection. Despite the consistent overlap, the weighted analysis showed that the size of clonotypes differed between the two compartments, indicating that these populations have a different clonotypic distribution, which probably reflects differing retention and expansion in different locations.

To better understand the magnitude of the observed repertoire overlaps, it is necessary to consider the size of the analyzed samples (10^3–10^5 cells) in comparison with the entire CD4$^+$ T cell repertoire (10^8 cells) in the human body, with the caveat of considering a fixed number of the most abundant clones in each subset. Importantly, it was observed that, when re-sampling exactly the same set of sequences *in silico* or by experimentally sequencing cells independently sorted from the same tissue sample, the repertoire overlap is never complete, and it decreases with increasing population diversity. These quantitative results suggest that the degree of overlap observed experimentally between separately sampled populations provides an underestimate of the considerable repertoire overlap between circulating and tTfh populations.

Extending the analysis to antigen-specific populations, we showed, using the T cell library technique (Geiger et al., 2009), that HA-specific CD4$^+$ T cells were enriched in the cTfh CXCR3$^+$ subset and the cNon-Tfh population, which contains the canonical CD4$^+$ Th1 subsets. The number of HA-specific clones generated from the cTfh CXCR3$^+$ and cNon-Tfh compartments was also much higher than that generated from the cTfh CXCR3$^-$ pool. The CD4$^+$CXCR3$^+$ bias in the HA-specific response is in line with previous reports (Palladino et al., 1991; Pedersen et al., 2014; Valkenburg et al., 2018; Velu et al., 2016; Yang et al., 2013; Yoon et al., 2018; Zielinski et al., 2011). Notably, in one of the 3 donors studied, the TCR sequences of blood-derived HA-specific cTfh CXCR3$^+$ clones were found in the tTfh CXCR3$^+$ repertoire, supporting a common clonal origin of antigen-specific Tfh cells in tonsils and the circulation. These results from analysis of antigen-specific cells provide strong support for the conclusions drawn from TCR deep sequencing: that the repertoires of cTfh and tTfh cells are very similar to each other but distinct from non-Tfh populations. Our observation of some repertoire sharing between Tfh GC and tTfh CXCR3$^+$ populations is consistent with the hypothesis that some of the cells participating in a GC reaction originate from the tTfh CXCR3$^+$ pool (Crotty, 2018; He et al., 2013). Whether a few Tfh GC cells, originally primed in a Th1 environment, are surviving to become memory Tfh Th1-like (or CXCR3$^+$) cells in the lymphoid organs and later in the periphery is not clear (Crotty, 2018). Tfh GC cells may revert, via a tTfh CXCR3$^-$ stage, to a tTfh CXCR3$^+$ phenotype

because we observed some modest repertoire overlap between all three of these tTfh populations as well as repertoire overlap unique to the tTfh CXCR3$^-$ and tTfh CXCR3$^+$ populations. These observations may apply to other Tfh cells with different phenotypes, similar to canonical Th cell subsets, but future work focusing on different pathogens that drive Th2 or Th17 responses is needed to elucidate this further.

Our TCR repertoire analysis also indicated very little overlap between antigen-experienced Tfh and non-Tfh cell populations in blood and tonsil tissues under steady-state conditions. This may suggest that these memory cells are derived from distinct clonal lineages, although it does not exclude the possibility that memory CD4$^+$ T cells, which are known to exhibit plasticity (Becattini et al., 2014; Caza and Landas, 2015; Hegazy et al., 2010; O'Shea et al., 2010), may alter their phenotype and become Tfh cells during an acute immune response (Boyden et al., 2012; Pepper et al., 2011). However, given that only the top2000 most abundant clonotypes in each population were compared, we cannot preclude that clones that were more highly expanded in the Tfh compartment were not also present at low frequency in the non-Tfh compartment and vice versa. Nonetheless, there were substantial differences in the TCR repertoires of antigen-experienced Tfh and non-Tfh populations. Furthermore, when studying influenza virus-specific cells (in the absence of a current influenza infection), we found that the peptides recognized by HA-specific CD4$^+$ T cell clones showed a wide diversity of specificities, and there was a surprisingly small overlap in the peptides recognized by Tfh and non-Tfh subsets. The distinction between Tfh and non-Tfh subsets in peripheral blood was uniquely confirmed by the combination of TCR sequencing and peptide specificity testing for cTfh CXCR3$^+$, cTfh CXCR3$^-$, and cNon-Tfh HA-reactive T cell clones; the results indicated that these cells were generated from different naive clones. Future studies should explore the differences between repertoires of Tfh and non-Tfh cells in blood and GC over the course of acute responses to infection or vaccination.

Non-Tfh cells constitute the majority of the CD4$^+$ T cell population in the blood (PD-1$^+$CXCR5$^+$ cTfh cells comprise only 15% of memory and 6% of total blood CD4$^+$ T cells), and, for many years, measurement of total CD4$^+$ T cell responses in PBMCs has been used to assess the magnitude of helper T cell responses in the context of B cell and antibody responses. Our findings show that evaluation of the overall antigen-specific CD4$^+$ T cell response will not give an accurate picture of the response in the Tfh compartment. There was very little clonal overlap between *bona fide* helper Tfh cells, particularly Tfh GC cells, and CXCR5$^-$CD4$^+$ memory T cells in the blood or tonsils, and there were marked differences in the epitope specificity of HA-reactive cTfh and cNon-Tfh cells. However, there were significant overlaps between the CXCR5$^+$ Tfh populations in the blood and Tfh cells in lymphoid tissues. Therefore, to investigate the specificity of true Tfh responses, it will be necessary to identify circulating Tfh cells and to study their antigen reactivity. These findings have important implications for evaluating the breadth and specificity of immune responses in clinical trials of vaccines aimed at stimulating protective antibody responses.

STAR★METHODS

Detailed methods are provided in the online version of this paper and include the following:

- KEY RESOURCES TABLE
- LEAD CONTACT AND MATERIALS AVAILABILITY
- EXPERIMENTAL MODEL AND SUBJECT DETAILS
  - Human studies
- METHOD DETAILS
  - Human sample processing
  - Phenotypic analysis and intracellular cytokine staining
  - CD4$^+$ T cell library
  - Antigen-specific CD4$^+$ T cell clones
  - Peptide-mapping of antigen-specific CD4$^+$ T cell clones
  - TCR deep-sequencing
  - TCR sequencing of antigen-specific CD4$^+$ T cell clones
  - Quantification of influenza-specific IgG
- QUANTIFICATION AND STATISTICAL ANALYSIS
  - Flow cytometry data
  - TCR deep-sequencing analysis
  - Bootstrap method
  - T cell library analysis
  - Antigen-specific CD4$^+$ T cell frequencies
- DATA AND CODE AVAILABILITY

SUPPLEMENTAL INFORMATION

Supplemental Information can be found online at https://doi.org/10.1016/j.celrep.2019.12.016.

ACKNOWLEDGMENTS

We thank the donors for their willing participation in this study, research nurses Deborah Barker and Dawn Young, the surgical team at the John Radcliffe Hospital in Oxford, and Stephen C. Harrison (Harvard University) for providing the hemagglutinin protein (Wisconsin strain). This work was supported by the National Institute of Allergy and Infectious Diseases at the National Institutes of Health (NIH) (Duke Centre for HIV/AIDS Vaccine Immunology-Immunogen Discovery grant UM1 AI 00645 and Duke Consortium for HIV/AIDS Vaccine Development grant UM1 AI144371), the Medical Research Council (MR/K012037), the Wellcome Trust (100326/Z/12/Z), and the Ministry of Science and Higher Education of the Russian Federation (075-15-2019-1789). P. Borrow, A.J.M., T.L., and S.C.G. are Jenner Institute Investigators. D.A.P. is a Wellcome Trust Senior Investigator.

AUTHOR CONTRIBUTIONS

E.B. performed and designed the experiments, analyzed the data, and wrote the first draft of the manuscript with supervision and support from S.L.C., P. Borrow, and A.J.M. A.N.D. and M.M. performed TCR sequencing and data analysis with help and supervision from D.M.C. K.L. and J.E.M. performed TCR sequencing and data analysis with help and supervision from D.A.P. T.L. and S.C.G. set up and obtained ethical approval for the clinical study. J.D.R. led the clinical team and performed tonsillectomies. P. Bonaiuti performed statistical analyses and assisted E.B. with data analysis. P. Borrow and A.J.M. directed and supervised the project and edited the manuscript. All authors contributed intellectually and read and approved the final version of the manuscript.

DECLARATION OF INTERESTS

The authors declare no competing interests.

Received: June 21, 2019
Revised: September 16, 2019
Accepted: December 5, 2019
Published: January 7, 2020

REFERENCES

Alam, S., and Sant, A.J. (2011). Infection with seasonal influenza virus elicits CD4 T cells specific for genetically conserved epitopes that can be rapidly mobilized for protective immunity to pandemic H1N1 influenza virus. J. Virol. *85*, 13310–13321.

Ansel, K.M., Ngo, V.N., Hyman, P.L., Luther, S.A., Förster, R., Sedgwick, J.D., Browning, J.L., Lipp, M., and Cyster, J.G. (2000). A chemokine-driven positive feedback loop organizes lymphoid follicles. Nature *406*, 309–314.

Aschenbrenner, D., Foglierini, M., Jarrossay, D., Hu, D., Weiner, H.L., Kuchroo, V.K., Lanzavecchia, A., Notarbartolo, S., and Sallusto, F. (2018). An immunoregulatory and tissue-residency program modulated by c-MAF in human T_H17 cells. Nat. Immunol. *19*, 1126–1136.

Avery, D.T., Bryant, V.L., Ma, C.S., de Waal Malefyt, R., and Tangye, S.G. (2008). IL-21-induced isotype switching to IgG and IgA by human naive B cells is differentially regulated by IL-4. J. Immunol. *181*, 1767–1779.

Baumjohann, D., Preite, S., Reboldi, A., Ronchi, F., Ansel, K.M., Lanzavecchia, A., and Sallusto, F. (2013). Persistent antigen and germinal center B cells sustain T follicular helper cell responses and phenotype. Immunity *38*, 596–605.

Becattini, S., Latorre, D., Mele, F., Foglierini, M., De Gregorio, C., Cassotta, A., Fernandez, B., Kelderman, S., Schumacher, T.N., Corti, D., et al. (2014). Functional heterogeneity of human memory CD4+ T cell clones primed by pathogens or vaccines. Science *347*, 400–406.

Bentebibel, S., Lopez, S., Obermoser, G., Schmitt, N., Mueller, C., Harrod, C., Flano, E., Mejias, A., Albrecht, R.A., Blankenship, D., et al. (2013). Induction of ICOS+CXCR3+CXCR5+ TH cells correlates with antibody responses to influenza vaccination. Sci. Transl. Med. *5*, 176ra32.

Bolotin, D.A., Poslavsky, S., Mitrophanov, I., Shugay, M., Mamedov, I.Z., Putintseva, E.V., and Chudakov, D.M. (2015). MiXCR: software for comprehensive adaptive immunity profiling. Nat. Methods *12*, 380–381.

Boswell, K.L., Paris, R., Boritz, E., Ambrozak, D., Yamamoto, T., Darko, S., Wloka, K., Wheatley, A., Narpala, S., McDermott, A., et al. (2014). Loss of circulating CD4 T cells with B cell helper function during chronic HIV infection. PLoS Pathog. *10*, e1003853.

Bowyer, G., Grobbelaar, A., Rampling, T., Venkatraman, N., Morelle, D., Ballou, R.W., Hill, A.V.S., and Ewer, K.J. (2018). CXCR3+ T follicular helper cells induced by co-administration of RTS,S/AS01B and viral-vectored vaccines are associated with reduced immunogenicity and efficacy against malaria. Front. Immunol. *9*, 1660.

Boyden, A.W., Legge, K.L., and Waldschmidt, T.J. (2012). Pulmonary infection with influenza A virus induces site-specific germinal center and T follicular helper cell responses. PLoS ONE *7*, e40733.

Breitfeld, D., Ohl, L., Kremmer, E., Ellwart, J., Sallusto, F., Lipp, M., and Förster, R. (2000). Follicular B helper T cells express CXC chemokine receptor 5, localize to B cell follicles, and support immunoglobulin production. J. Exp. Med. *192*, 1545–1552.

Bryant, V.L., Ma, C.S., Avery, D.T., Li, Y., Good, K.L., Corcoran, L.M., de Waal Malefyt, R., and Tangye, S.G. (2007). Cytokine-mediated regulation of human B cell differentiation into Ig-secreting cells: predominant role of IL-21 produced by CXCR5+ T follicular helper cells. J. Immunol. *179*, 8180–8190.

Campion, S.L., Brodie, T.M., Fischer, W., Korber, B.T., Rossetti, A., Goonetilleke, N., McMichael, A.J., and Sallusto, F. (2014). Proteome-wide analysis of HIV-specific naive and memory CD4(+) T cells in unexposed blood donors. J. Exp. Med. *211*, 1273–1280.

Casamayor-Palleja, M., Khan, M., and MacLennan, I.C. (1995). A subset of CD4+ memory T cells contains preformed CD40 ligand that is rapidly but transiently expressed on their surface after activation through the T cell receptor complex. J. Exp. Med. *181*, 1293–1301.

Caza, T., and Landas, S. (2015). Functional and phenotypic plasticity of CD4(+) T cell subsets. BioMed Res. Int. *2015*, 521957.

Chevalier, N., Jarrossay, D., Ho, E., Avery, D.T., Ma, C.S., Yu, D., Sallusto, F., Tangye, S.G., and Mackay, C.R. (2011). CXCR5 expressing human central memory CD4 T cells and their relevance for humoral immune responses. J. Immunol. *186*, 5556–5568.

Choi, Y.S., Kageyama, R., Eto, D., Escobar, T.C., Johnston, R.J., Monticelli, L., Lao, C., and Crotty, S. (2011). ICOS receptor instructs T follicular helper cell versus effector cell differentiation via induction of the transcriptional repressor Bcl6. Immunity *34*, 932–946.

Colwell, R.K., Chao, A., Gotelli, N.J., Lin, S., Mao, C.X., Chazdon, R.L., and Longino, J.T. (2012). Models and estimators linking individual-based and sample-based rarefaction, extrapolation and comparison of assemblages. J. Plant Ecol. *5*, 3–21.

Crotty, S. (2014). T follicular helper cell differentiation, function, and roles in disease. Immunity *41*, 529–542.

Crotty, S. (2018). Do Memory CD4 T Cells Keep Their Cell-Type Programming: Plasticity versus Fate Commitment? Complexities of interpretation due to the heterogeneity of memory CD4 T Cells, including T follicular helper cells. Cold Spring Harb. Perspect. Biol. *10*, a032102.

Cubas, R., van Grevenynghe, J., Wills, S., Kardava, L., Santich, B.H., Buckner, C.M., Muir, R., Tardif, V., Nichols, C., Procopio, F., et al. (2015). Reversible reprogramming of circulating memory T follicular helper cell function during chronic HIV infection. J. Immunol. *195*, 5625–5636.

Dan, J.M., Havenar-Daughton, C., Kendric, K., Al-Kolla, R., Kaushik, K., Rosales, S.L., Anderson, E.L., LaRock, C.N., Vijayanand, P., Seumois, G., et al. (2019). Recurrent group A *Streptococcus* tonsillitis is an immunosusceptibility disease involving antibody deficiency and aberrant T_{FH} cells. Sci. Transl. Med. *11*, 1–11.

Day, C.L., Kaufmann, D.E., Kiepiela, P., Brown, J.A., Moodley, E.S., Reddy, S., Mackey, E.W., Miller, J.D., Leslie, A.J., DePierres, C., et al. (2006). PD-1 expression on HIV-specific T cells is associated with T-cell exhaustion and disease progression. Nature *443*, 350–354.

Djuretic, I.M., Levanon, D., Negreanu, V., Groner, Y., Rao, A., and Ansel, K.M. (2007). Transcription factors T-bet and Runx3 cooperate to activate Ifng and silence Il4 in T helper type 1 cells. Nat. Immunol. *8*, 145–153.

Dorfman, D.M., Brown, J.A., Shahsafaei, A., and Freeman, G.J. (2006). Programmed death-1 (PD-1) is a marker of germinal center-associated T cells and angioimmunoblastic T-cell lymphoma. Am. J. Surg. Pathol. *30*, 802–810.

Durand, M., Walter, T., Pirnay, T., Naessens, T., Gueguen, P., Goudot, C., Lameiras, S., Chang, Q., Talaei, N., Ornatsky, O., et al. (2019). Human lymphoid organ cDC2 and macrophages play complementary roles in T follicular helper responses. J. Exp. Med. *216*, 1561–1581.

Eren, M.I., Chao, A., Hwang, W.H., and Colwell, R.K. (2012). Estimating the richness of a population when the maximum number of classes is fixed: a nonparametric solution to an archaeological problem. PLoS ONE *7*, e34179.

Fazilleau, N., Eisenbraun, M.D., Malherbe, L., Ebright, J.N., Pogue-Caley, R.R., McHeyzer-Williams, L.J., and McHeyzer-Williams, M.G. (2007). Lymphoid reservoirs of antigen-specific memory T helper cells. Nat. Immunol. *8*, 753–761.

Förster, R., Mattis, A.E., Kremmer, E., Wolf, E., Brem, G., and Lipp, M. (1996). A putative chemokine receptor, BLR1, directs B cell migration to defined lymphoid organs and specific anatomic compartments of the spleen. Cell *87*, 1037–1047.

Geiger, R., Duhen, T., Lanzavecchia, A., and Sallusto, F. (2009). Human naive and memory CD4+ T cell repertoires specific for naturally processed antigens analyzed using libraries of amplified T cells. J. Exp. Med. *206*, 1525–1534.

Grivel, J.C., and Margolis, L. (2009). Use of human tissue explants to study human infectious agents. Nat. Protoc. *4*, 256–269.

Groom, J.R., and Luster, A.D. (2011). CXCR3 in T cell function. Exp. Cell Res. *317*, 620–631.

Hale, J.S., and Ahmed, R. (2015). Memory T follicular helper CD4 T cells. Front. Immunol. *6*, 16.

Hansen, D.S., Obeng-Adjei, N., Ly, A., Ioannidis, L.J., and Crompton, P.D. (2017). Emerging concepts in T follicular helper cell responses to malaria. Int. J. Parasitol. *47*, 105–110.

Harrell, F.E. (2001). Regression Modeling Strategies With Applications To Linear Models, Logistic Regression, and Survival Analysis (Springer).

Havenar-Daughton, C., Carnathan, D.G., Torrents de la Peña, A., Pauthner, M., Briney, B., Reiss, S.M., Wood, J.S., Kaushik, K., van Gils, M.J., Rosales, S.L., et al. (2016). Direct probing of germinal center responses reveals immunological features and bottlenecks for neutralizing antibody responses to HIV Env trimer. Cell Rep. *17*, 2195–2209.

Haynes, N.M., Allen, C.D.C., Lesley, R., Ansel, K.M., Killeen, N., and Cyster, J.G. (2007). Role of CXCR5 and CCR7 in follicular Th cell positioning and appearance of a programmed cell death gene-1high germinal center-associated subpopulation. J. Immunol. *179*, 5099–5108.

He, J., Tsai, L.M., Leong, Y.A., Hu, X., Ma, C.S., Chevalier, N., Sun, X., Vandenberg, K., Rockman, S., Ding, Y., et al. (2013). Circulating precursor CCR7(lo) PD-1(hi) CXCR5^{+} CD4^{+} T cells indicate Tfh cell activity and promote antibody responses upon antigen reexposure. Immunity *39*, 770–781.

Heather, J.M., Ismail, M., Oakes, T., and Chain, B. (2018). High-throughput sequencing of the T-cell receptor repertoire: pitfalls and opportunities. Brief. Bioinform. *19*, 554–565.

Hegazy, A.N., Peine, M., Helmstetter, C., Panse, I., Fröhlich, A., Bergthaler, A., Flatz, L., Pinschewer, D.D., Radbruch, A., and Löhning, M. (2010). Interferons direct Th2 cell reprogramming to generate a stable GATA-3(+)T-bet(+) cell subset with combined Th2 and Th1 cell functions. Immunity *32*, 116–128.

Heit, A., Schmitz, F., Gerdts, S., Flach, B., Moore, M.S., Perkins, J.A., Robins, H.S., Aderem, A., Spearman, P., Tomaras, G.D., et al. (2017). Vaccination establishes clonal relatives of germinal center T cells in the blood of humans. J. Exp. Med. *214*, 2139–2152.

Herati, R.S., Muselman, A., Vella, L., Bengsch, B., Parkhouse, K., Alcazar, D., Del, Kotzin, J., Doyle, S.A., Tebas, P., Hensley, S.E., et al. (2017). Successive annual influenza vaccination induces a recurrent oligoclonotypic memory response in circulating T follicular helper cells. Sci. Immunol. *2*, eaag2152.

Hill, D.L., Pierson, W., Bolland, D.J., Mkindi, C., Carr, E.J., Wang, J., Houard, S., Wingett, S.W., Audran, R., Wallin, E.F., et al. (2019). The adjuvant GLA-SE promotes human Tfh cell expansion and emergence of public TCRβ clonotypes. J. Exp. Med. *216*, 1857–1873.

Izraelson, M., Nakonechnaya, T.O., Moltedo, B., Egorov, E.S., Kasatskaya, S.A., Putintseva, E.V., Mamedov, I.Z., Staroverov, D.B., Shemiakina, I.I., Zakharova, M.Y., et al. (2018). Comparative analysis of murine T-cell receptor repertoires. Immunology *153*, 133–144.

Kim, C.H., Rott, L.S., Clark-Lewis, I., Campbell, D.J., Wu, L., and Butcher, E.C. (2001). Subspecialization of CXCR5+ T cells: B helper activity is focused in a germinal center-localized subset of CXCR5+ T cells. J. Exp. Med. *193*, 1373–1381.

Lefranc, M.P. (2003). IMGT, the international ImMunoGeneTics database. Nucleic Acids Res. *31*, 307–310.

Lindestam Arlehamn, C.S., Gerasimova, A., Mele, F., Henderson, R., Swann, J., Greenbaum, J.A., Kim, Y., Sidney, J., James, E.A., Taplitz, R., et al. (2013). Memory T cells in latent Mycobacterium tuberculosis infection are directed against three antigenic islands and largely contained in a CXCR3+CCR6+ Th1 subset. PLoS Pathog. *9*, e1003130.

Liu, Y.J., Joshua, D.E., Williams, G.T., Smith, C.A., Gordon, J., and MacLennan, I.C.M. (1989). Mechanism of antigen-driven selection in germinal centres. Nature *342*, 929–931.

Locci, M., Havenar-Daughton, C., Landais, E., Wu, J., Kroenke, M.A., Arlehamn, C.L., Su, L.F., Cubas, R., Davis, M.M., Sette, A., et al.; International AIDS Vaccine Initiative Protocol C Principal Investigators (2013). Human circulating PD-1+CXCR3-CXCR5+ memory Tfh cells are highly functional and correlate with broadly neutralizing HIV antibody responses. Immunity *39*, 758–769.

Locci, M., Wu, J.E., Arumemi, F., Mikulski, Z., Dahlberg, C., Miller, A.T., and Crotty, S. (2016). Activin A programs the differentiation of human TFH cells. Nat. Immunol. *17*, 976–984.

Ma, C.S., Suryani, S., Avery, D.T., Chan, A., Nanan, R., Santner-Nanan, B., Deenick, E.K., and Tangye, S.G. (2009). Early commitment of naïve human CD4(+) T cells to the T follicular helper (T(FH)) cell lineage is induced by IL-12. Immunol. Cell Biol. *87*, 590–600.

Mele, F., Fornara, C., Jarrossay, D., Furione, M., Arossa, A., Spinillo, A., Lanzavecchia, A., Gerna, G., Sallusto, F., and Lilleri, D. (2017). Phenotype and specificity of T cells in primary human cytomegalovirus infection during pregnancy: IL-7Rpos long-term memory phenotype is associated with protection from vertical transmission. PLoS ONE *12*, e0187731.

Miura, K., Orcutt, A.C., Muratova, O.V., Miller, L.H., Saul, A., and Long, C.A. (2008). Development and characterization of a standardized ELISA including a reference serum on each plate to detect antibodies induced by experimental malaria vaccines. Vaccine *26*, 193–200.

Morita, R., Schmitt, N., Bentebibel, S.E., Ranganathan, R., Bourdery, L., Zurawski, G., Foucat, E., Dullaers, M., Oh, S., Sabzghabaei, N., et al. (2011). Human blood CXCR5(+)CD4(+) T cells are counterparts of T follicular cells and contain specific subsets that differentially support antibody secretion. Immunity *34*, 108–121.

Nurieva, R.I., Chung, Y., Hwang, D., Yang, X.O., Kang, H.S., Ma, L., Wang, Y.H., Watowich, S.S., Jetten, A.M., Tian, Q., and Dong, C. (2008). Generation of T follicular helper cells is mediated by interleukin-21 but independent of T helper 1, 2, or 17 cell lineages. Immunity *29*, 138–149.

O'Shea, J.J.O., Cells, C.D.T., and Paul, W.E. (2010). Mechanisms underlying lineage commitment and plasticity of helper CD4+ T cells. Science *327*, 1098–1102.

Obeng-Adjei, N., Portugal, S., Tran, T.M., Yazew, T.B., Skinner, J., Li, S., Jain, A., Felgner, P.L., Doumbo, O.K., Kayentao, K., et al. (2015). Circulating Th1-Cell-type Tfh cells that exhibit impaired B cell help are preferentially activated during acute malaria in children. Cell Rep. *13*, 425–439.

Palladino, G., Scherle, P.A., and Gerhard, W. (1991). Activity of CD4+ T-cell clones of type 1 and type 2 in generation of influenza virus-specific cytotoxic responses in vitro. J. Virol. *65*, 6071–6076.

Pallikkuth, S., Parmigiani, A., Silva, S.Y., George, V.K., Fischl, M., Pahwa, R., and Pahwa, S. (2012). Impaired peripheral blood T-follicular helper cell function in HIV-infected nonresponders to the 2009 H1N1/09 vaccine. Blood *120*, 985–993.

Pedersen, G.K., Sjursen, H., Nøstbakken, J.K., Jul-Larsen, Å., Hoschler, K., and Cox, R.J. (2014). Matrix M(^{TM}) adjuvanted virosomal H5N1 vaccine induces balanced Th1/Th2 CD4(+) T cell responses in man. Hum. Vaccin. Immunother. *10*, 2408–2416.

Pepper, M., Pagán, A.J., Igyártó, B.Z., Taylor, J.J., and Jenkins, M.K. (2011). Opposing signals from the Bcl6 transcription factor and the interleukin-2 receptor generate T helper 1 central and effector memory cells. Immunity *35*, 583–595.

Ploquin, M.J.Y., Eksmond, U., and Kassiotis, G. (2011). B cells and TCR avidity determine distinct functions of CD4+ T cells in retroviral infection. J. Immunol. *187*, 3321–3330.

Precopio, M.L., Butterfield, T.R., Casazza, J.P., Little, S.J., Richman, D.D., Koup, R.A., and Roederer, M. (2008). Optimizing peptide matrices for identifying T-cell antigens. Cytometry A *73*, 1071–1078.

Price, D.A., Brenchley, J.M., Ruff, L.E., Betts, M.R., Hill, B.J., Roederer, M., Koup, R.A., Migueles, S.A., Gostick, E., Wooldridge, L., et al. (2005). Avidity for antigen shapes clonal dominance in CD8+ T cell populations specific for persistent DNA viruses. J. Exp. Med. *202*, 1349–1361.

Quigley, M.F., Almeida, J.R., Price, D.A., and Douek, D.C. (2011). Unbiased molecular analysis of T Cell receptor expression using template-switch anchored RT-PCR. Curr. Protoc. Immunol. *Chapter 10*, Unit 10.33.

Reinhardt, R.L., Liang, H.E., and Locksley, R.M. (2009). Cytokine-secreting follicular T cells shape the antibody repertoire. Nat. Immunol. *10*, 385–393.

Rosati, E., Dowds, C.M., Liaskou, E., Henriksen, E.K.K., Karlsen, T.H., and Franke, A. (2017). Overview of methodologies for T-cell receptor repertoire analysis. BMC Biotechnol. *17*, 61.

Ryg-Cornejo, V., Ioannidis, L.J., Ly, A., Chiu, C.Y., Tellier, J., Hill, D.L., Preston, S.P., Pellegrini, M., Yu, D., Nutt, S.L., et al. (2016). Severe malaria infections impair germinal center responses by inhibiting T follicular helper cell differentiation. Cell Rep. *14*, 68–81.

Sallusto, F., Cassotta, A., Hoces, D., Foglierini, M., and Lanzavecchia, A. (2018). Do Memory CD4 T Cells Keep Their Cell-Type Programming: Plasticity versus Fate Commitment? T-Cell heterogeneity, plasticity, and selection in humans. Cold Spring Harb. Perspect. Biol. *10*, a029421.

Sant, A.J., DiPiazza, A.T., Nayak, J.L., Rattan, A., and Richards, K.A. (2018). CD4 T cells in protection from influenza virus: Viral antigen specificity and functional potential. Immunol. Rev. *284*, 91–105.

Schaerli, P., Willimann, K., Lang, A.B., Lipp, M., Loetscher, P., and Moser, B. (2000). CXC chemokine receptor 5 expression defines follicular homing T cells with B cell helper function. J. Exp. Med. *192*, 1553–1562.

Shi, J., Hou, S., Fang, Q., Liu, X., Liu, X., and Qi, H. (2018). PD-1 controls follicular T helper cell positioning and function. Immunity *49*, 264–274.e4.

Shugay, M., Bolotin, D.A., Putintseva, E.V., Pogorelyy, M.V., Mamedov, I.Z., and Chudakov, D.M. (2013). Huge overlap of individual TCR beta repertoires. Front. Immunol. *4*, 466.

Shugay, M., Britanova, O.V., Merzlyak, E.M., Turchaninova, M.A., Mamedov, I.Z., Tuganbaev, T.R., Bolotin, D.A., Staroverov, D.B., Putintseva, E.V., Plevova, K., et al. (2014). Towards error-free profiling of immune repertoires. Nat. Methods *11*, 653–655.

Shugay, M., Bagaev, D.V., Turchaninova, M.A., Bolotin, D.A., Britanova, O.V., Putintseva, E.V., Pogorelyy, M.V., Nazarov, V.I., Zvyagin, I.V., Kirgizova, V.I., et al. (2015). VDJtools: unifying post-analysis of T cell receptor repertoires. PLoS Comput. Biol. *11*, e1004503.

Tew, J.G., and Mandel, T.E. (1979). Prolonged antigen half-life in the lymphoid follicles of specifically immunized mice. Immunology *37*, 69–76.

Tew, J.G., Mandel, T.E., Phipps, R.P., and Szakal, A.K. (1984). Tissue localization and retention of antigen in relation to the immune response. Am. J. Anat. *170*, 407–420.

Valkenburg, S.A., Li, O.T.W., Li, A., Bull, M., Waldmann, T.A., Perera, L.P., Peiris, M., and Poon, L.L.M. (2018). Protection by universal influenza vaccine is mediated by memory CD4 T cells. Vaccine *36*, 4198–4206.

Vella, L.A., Buggert, M., Manne, S., Herati, R.S., Sayin, I., Kuri-Cervantes, L., Bukh Brody, I., O'Boyle, K.C., Kaprielian, H., Giles, J.R., et al. (2019). T follicular helper cells in human efferent lymph retain lymphoid characteristics. J. Clin. Invest. *129*, 3185–3200.

Velu, V., Mylvaganam, G.H., Gangadhara, S., Hong, J.J., Iyer, S.S., Gumber, S., Ibegbu, C.C., Villinger, F., and Amara, R.R. (2016). Induction of Th1-biased T follicular helper (Tfh) cells in lymphoid tissues during chronic simian immunodeficiency virus infection defines functionally distinct germinal center Tfh cells. J. Immunol. *197*, 1832–1842.

Vinuesa, C.G., Tangye, S.G., Moser, B., and Mackay, C.R. (2005). Follicular B helper T cells in antibody responses and autoimmunity. Nat. Rev. Immunol. *5*, 853–865.

Vinuesa, C.G., Linterman, M.A., Yu, D., and MacLennan, I.C.M. (2016). Follicular helper T cells. Annu. Rev. Immunol. *34*, 335–368.

Weber, J.P., Fuhrmann, F., Feist, R.K., Lahmann, A., Al Baz, M.S., Gentz, L.J., Vu Van, D., Mages, H.W., Haftmann, C., Riedel, R., et al. (2015). ICOS maintains the T follicular helper cell phenotype by down-regulating Krüppel-like factor 2. J. Exp. Med. *212*, 217–233.

Wong, M.T., Ong, D.E.H., Lim, F.S.H., Teng, K.W.W., McGovern, N., Narayanan, S., Ho, W.Q., Cerny, D., Tan, H.K.K., Anicete, R., et al. (2016). A High-dimensional atlas of human T cell diversity reveals tissue-specific trafficking and cytokine signatures. Immunity *45*, 442–456.

Xu, H., Li, X., Liu, D., Li, J., Zhang, X., Chen, X., Hou, S., Peng, L., Xu, C., Liu, W., et al. (2013). Follicular T-helper cell recruitment governed by bystander B cells and ICOS-driven motility. Nature *496*, 523–527.

Yang, J., James, E., Gates, T.J., DeLong, J.H., LaFond, R.E., Malhotra, U., and Kwok, W.W. (2013). CD4+ T cells recognize unique and conserved 2009 H1N1 influenza hemagglutinin epitopes after natural infection and vaccination. Int. Immunol. *25*, 447–457.

Yoon, S.W., Wong, S.S., Zhu, H., Chen, R., Li, L., Zhang, Y., Guan, Y., and Webby, R.J. (2018). Dysregulated T-helper type 1 (Th1):Th2 cytokine profile and poor immune response in pregnant ferrets infected with 2009 pandemic influenza A(H1N1) virus. J. Infect. Dis. *217*, 438–442.

Yusuf, I., Kageyama, R., Monticelli, L., Johnston, R.J., Ditoro, D., Hansen, K., Barnett, B., and Crotty, S. (2010). Germinal center T follicular helper cell IL-4 production is dependent on signaling lymphocytic activation molecule receptor (CD150). J. Immunol. *185*, 190–202.

Zielinski, C.E., Corti, D., Mele, F., Pinto, D., Lanzavecchia, A., and Sallusto, F. (2011). Dissecting the human immunologic memory for pathogens. Immunol. Rev. *240*, 40–51.

STAR★METHODS

KEY RESOURCES TABLE

REAGENT or RESOURCE	SOURCE	IDENTIFIER
Antibodies		
Anti-human CD3 Brilliant Violet 605	Becton Dickinson	Cat#742623; RRID: AB_2740919
Live/Dead Fixable Aqua	Invitrogen	Cat#L34957
Anti-human CD4 APC-Cy7	Becton Dickinson	Cat#557871; RRID: AB_396913
Anti-human CD45RA PE-TexasRed	Invitrogen	Cat#MHCD45RA17; RRID: AB_1476948
Anti-human CXCR3 PE-Cy5	Becton Dickinson	Cat#551128; RRID: AB_394061
Anti-human CXCR5 Alexa Fluor 488	Becton Dickinson	Cat#558112; RRID: AB_397034
Anti-human ICOS Brilliant Violet 711	Becton Dickinson	Cat#563833; RRID: AB_2738440
Anti-human ICOS PE	BioLegend	Cat#313508; RRID: AB_416332
Anti-human PD-1 Brilliant Violet 421	Becton Dickinson	Cat#562516; RRID: AB_11153482
Anti-human CD8 PE-Cy7	Becton Dickinson	Cat#335822
Anti-human CD14 FITC	Becton Dickinson	Cat#555397; RRID: AB_395798
Anti-human CD14 PE-Cy7	Becton Dickinson	Cat#557742; RRID: AB_396848
Anti-human CD16 PE-Cy7	Becton Dickinson	Cat#557744; RRID: AB_396850
Anti-human CD19 PE-Cy7	Becton Dickinson	Cat#557835; RRID: AB_396893
Anti-human CD25 PE-Cy7	Becton Dickinson	Cat#335824
Anti-human CD56 PE-Cy7	Becton Dickinson	Cat#557747; RRID: AB_396853
Anti-human IFN-gamma Alexa Fluor 700	Becton Dickinson	Cat#557995; RRID: AB_396977
Anti-human IL-4 PE	Becton Dickinson	Cat#554485; RRID: AB_395424
Anti-human IL-21 Alexa Fluor 647	Becton Dickinson	Cat#560493; RRID: AB_1645421
Biological Samples		
Peripheral blood of adults individual undergoing tonsillectomy	JR Hospital, Oxford, UK	LABFLU002
Tonsil samples of adults	JR Hospital, Oxford, UK	LABFLU002
Cone samples from peripheral blood of healthy individuals	UK National Blood Service	N/A
Chemicals, Peptides, and Recombinant Proteins		
Haemagglutinin protein	Prof Stephen Harrison (Harvard Medical School, MA)	Influenza A Wisconsin/67/2005
Overlapping peptides of Haemagglutinin protein	GenScript	Influenza A California/04/2009
Haemagglutinin protein	BEI Resources	Influenza A/California/04/2009
Commercial Trivalent Influenza Vaccine	Sanofi Pasteur	Split Virion, Inactivated
Phytohemagglutinin purified	Remel	R30852801
Critical Commercial Assays		
Human TCR Profiling Kit	MiLaboratory LLC	N/A
NextSeq 500/550 High Output Kit v2.5 (300 Cycles)	Illumina	20024908
RNeasy micro kit	QIAGEN	74004
Deposited Data		
TCR sequencing data	Mendely Data	https://doi.org/10.17632/wry2ddh8zx.1
Oligonucleotides		
Primer MAC2 GGAACTTTCTGGGCTGGGGAAGAAGGTGT CTTCTGG	Quigley et al., 2011	N/A
Primer MBC2 TGCTTCTGATGGCTCAAACACAGCGACCT	Quigley et al., 2011	N/A
Primer M13 Forward: TTTTCCCAGTCACGAC	Invitrogen	N/A
Primer M13 Reverse: CAGGAAACAGCTATGAC	Invitrogen	N/A

(*Continued on next page*)

Continued

REAGENT or RESOURCE	SOURCE	IDENTIFIER
Software and Algorithms		
MIGEC	https://milaboratory.com/software/	MiLaboratory LLC
MiXCR	https://milaboratory.com/software/	MiLaboratory LLC
VDJtools	https://milaboratory.com/software/	MiLaboratory LLC
Cytoscape	https://cytoscape.org/	Cytoscape Version 3.6.1
Open Gen5	BioTek	N/A

LEAD CONTACT AND MATERIALS AVAILABILITY

This study did not generate new unique reagents. Further information and requests for resources and reagents should be directed to and will be fulfilled by the Lead Contact, Andrew J. McMichael (andrew.mcmichael@ndm.ox.ac.uk).

EXPERIMENTAL MODEL AND SUBJECT DETAILS

Human studies

Volunteer adult donors (16–50 years old) admitted for elective tonsillectomy at the John Radcliffe Hospital in Oxford because of a history of recurrent tonsillitis or sleep apnea consented to donate peripheral blood (80–100 mL) on the day of the surgery (Table S6). Tonsillectomy was performed in the absence of acute infection. Patients were excluded from the study if they were affected by immunodeficiency, serious ongoing infection (e.g., hepatitis B, hepatitis C or HIV infection or other infections deemed by the investigators to impact on the study), lymphoid malignancy, cytogenetic disorders, history of cancer, any pre-existing heart disease or a blood clotting disorder. The existing LABFLU002 clinical protocol was amended to cover these studies and was ethically approved by the Oxford B Research Ethics Committee (13/SC/0152). Written informed consent was obtained from all subjects in accordance with the Declaration of Helsinki. Peripheral blood samples for T cell library interrogations were collected from healthy donors via the UK National Blood Service.

METHOD DETAILS

Human sample processing

Tonsil nodules from adult donors were collected within 4 h of surgery into RPMI 1640 glutamine [-] medium (Invitrogen) supplemented with non-essential amino acids (1%, Invitrogen), sodium pyruvate (1%, Invitrogen), glutamine (1%, Invitrogen), pooled AB human sera (5%, UK National Blood Service), β-mercaptoethanol (0.1%, Invitrogen) and penicillin/streptomycin (1%, Invitrogen). All samples were kept on ice during transportation. Tonsillar tissues were cleared from fatty and necrotic areas and cut into sections at a thickness of 2–3 mm using scalpels and scissors. The sections were then passed through a 70 μm cell strainer and filtered through a 40 μm cell strainer (Grivel and Margolis, 2009). Manually processed tonsils and peripheral blood samples were diluted 1:2 with Hank's Balanced Salt Solution (Sigma-Aldrich) and layered over 20 mL of Histopaque-1077 (Sigma-Aldrich). Mononuclear cells were isolated via density gradient centrifugation (800 g for 30 min). Flow cytometric analyses of phenotypic markers were performed directly *ex vivo*. $CD14^+$ cells were enriched from PBMCs via magnetic separation using CD14 MicroBeads (Miltenyi Biotec).

Phenotypic analysis and intracellular cytokine staining

Mononuclear cells from tonsil and blood samples were washed in Dulbecco's PBS (Sigma-Aldrich). For phenotypic analyses, cells were labeled with Live/Dead Fixable Aqua and surface stained with anti-CD4–APC-Cy7, anti-CD45RA–PE-TxRed, anti-CXCR3–PE-Cy5, anti-CXCR5–AF488, anti-ICOS–BV711, anti-PD-1–BV421 and the dump markers anti-CD8, anti-CD14, anti-CD16, anti-CD19, anti-CD25 and anti-CD56 (all conjugated to PE-Cy7) for 15 min at 37°C (reagent details in Key Resources Table). For cytokine production, cells were stimulated with phorbol 12-myristate 13-acetate (2×10^{-7} M, Sigma-Aldrich) and ionomycin (1 μg/mL, Sigma-Aldrich) for 5 hr at 37°C. Brefeldin A was added after 2 hr (10 μg/mL, Sigma-Aldrich). Cells were then surface stained as described above, fixed/permeabilized with Cytofix/Cytoperm 1X Solution (BD PharMingen), and stained in Permwash 1X Solution (BD PharMingen) with anti-CD4–APC-Cy7, anti-IFN-γ–AF700, anti-IL-4–PE and anti-IL-21–AF647 for 20 min on ice (reagent details in Key Resources Table). The flow cytometry panel was internally validated using individually stained CompBeads (BD Biosciences). Stained samples were acquired using an LSR Fortessa (BD Biosciences) and analyzed using FlowJo software v10.3 (Tree Star).

$CD4^+$ T cell library

$CD4^+$ and $CD14^+$ cells were enriched from the PBMCs of 3 healthy donors via magnetic separation using the corresponding MicroBeads (Miltenyi Biotec). The $CD14^+$ fraction was cryopreserved in liquid nitrogen. $CD4^+$ T cells were stained with Live/Dead

Fixable Aqua, anti-CD3–BV605, anti-CD4–APC-Cy7, anti-CD45RA–PE-TxRed, anti-CXCR3–PE-Cy5, anti-CXCR5–AF488, anti-PD-1–BV421 and the dump markers anti-CD8, anti-CD14, anti-CD16, anti-CD19, anti-CD25 and anti-CD56 (all conjugated to PE-Cy7) for 15 min at 37°C (reagent details in Key Resources Table). Circulating live $CD3^+CD4^+CD45RA^-$ cells were sorted into cTfh $CXCR3^+$ ($CXCR3^+CXCR5^+PD\text{-}1^+$), cTfh $CXCR3^-$ ($CXCR3^-CXCR5^+PD\text{-}1^+$) and cNon-Tfh ($CXCR5^-$) subsets using a FACSAria III (BD Biosciences). Sorting was performed using a 4-way purity to obtain 3–5x10^5 cells per subset at a minimum purity of 92%. Sorted $CD4^+$ T cells were seeded at a limiting dilution of 1 × 10^4 cells/mL in RPMI 1640 glutamine [-] medium (Invitrogen) supplemented with non-essential amino acids (1%, Invitrogen), sodium pyruvate (1%, Invitrogen), glutamine (1%, Invitrogen), pooled AB human sera (5%, UK National Blood Service), β-mercaptoethanol (0.1%, Invitrogen), penicillin/streptomycin (1%, Invitrogen) and IL-2 (500 U/mL, University of Oxford). Cells were expanded with 1 μg/mL phytohemagglutinin (Remel) in the presence of irradiated (45 Gy) allogeneic feeder cells from 3 different healthy blood donors (10^6 feeder cells/mL). After 20 days, each line was screened for the capacity to proliferate in response to HA protein. Autologous $CD14^+$ monocytes were irradiated at 45 Gy and incubated (3 × 10^5 cells/mL) for 5 hr at 37°C with HA protein (5 μg/mL) from Influenza A Wisconsin/67/2005 (a gift from Professor Stephen Harrison, Harvard Medical School). Negative control wells incorporated dimethyl sulfoxide (0.045%, Sigma-Aldrich), and positive control wells incorporated IL-2 (500 U/mL, University of Oxford). An aliquot of 2.5 × 10^6 cells/mL from each expanded $CD4^+$ T cell line was added to the monocytes after washing and resting in fresh culture medium without IL-2 for 5 hr. After 3 days, 1 μCi/mL [^{3}H]-thymidine was added to the cultures, and proliferation was measured after 16 hr using a MicroBeta2 Counter (Perkin Elmer) (Campion et al., 2014; Geiger et al., 2009; Lindestam Arlehamn et al., 2013; Mele et al., 2017).

Antigen-specific $CD4^+$ T cell clones

Frozen CD14-depleted PBMCs were defrosted and rested overnight at 37°C in RPMI 1640 glutamine [-] medium (Invitrogen) supplemented with non-essential amino acids (1%, Invitrogen), sodium pyruvate (1%, Invitrogen), glutamine (1%, Invitrogen), pooled AB human sera (10%, UK National Blood Service), β-mercaptoethanol (0.1%, Invitrogen) and penicillin/streptomycin (1%, Invitrogen). $CD4^+$ cells were enriched via magnetic separation using CD4 MicroBeads (Miltenyi Biotec) and surface stained as described above. Among live lymphocytes, circulating $CD3^+CD4^+CD45RA^-$ cells were sorted into cTfh $CXCR3^+$ ($CXCR3^+CXCR5^+PD\text{-}1^+$), cTfh $CXCR3^-$ ($CXCR3^-CXCR5^+PD\text{-}1^+$) and cNon-Tfh ($CXCR5^-$) subsets using a FACS Aria III (BD Biosciences). Sorted subsets (3x10^6 cells/mL) were stimulated at a 3:1 ratio with irradiated (45 Gy) autologous $CD14^+$ monocytes loaded as described above with overlapping HA peptides (2 μg/mL) corresponding to Influenza A California/04/2009 (GenScript). Peptides were 14–18 amino acids long with a 12 residue overlap spanning the entire length of HA. After 7 days, cells were stained with Live/Dead Fixable Aqua, anti-CD3–BV605, anti-CD4–APC-Cy7, anti-CD25–PE-Cy7, anti-CD45RA–PE-TxRed, anti-ICOS–PE and the dump marker anti-CD14 (conjugated to FITC) for 15 min at 37°C (reagent details in Key Resources Table). Activated $CD4^+$ T cells ($CD3^+CD4^+CD14^-CD25^+ICOS^+$) were sorted using a FACSAria III (BD Biosciences) and seeded at 0.4 cells/well into 384-well plates (Corning). Cells were expanded with phytohemagglutinin (1 μg/mL, Remel) in the presence of irradiated (45 Gy) allogeneic feeder cells from 3 different healthy blood donors (10^6 feeder cells/mL) in RPMI 1640 glutamine [-] medium (Invitrogen) supplemented with non-essential amino acids (1%, Invitrogen), sodium pyruvate (1%, Invitrogen), glutamine (1%, Invitrogen), pooled AB human sera (10%, UK National Blood Service), β-mercaptoethanol (0.1%, Invitrogen), penicillin/streptomycin (1%, Invitrogen) and IL-2 (500 U/mL, University of Oxford). After 14 days, T cell clones were identified and transferred into 96-well round-bottom plates (Corning). To confirm specificity, an aliquot of each clone (1 × 10^6 cells/mL) was stimulated with the relevant overlapping peptide pool (2 μg/mL) after washing and resting in fresh culture medium without IL-2 for 5 hr. After 3 days, 1 μCi/mL [^{3}H]-thymidine was added to the cultures, and proliferation was measured after 16 hr using a MicroBeta2 Counter (Perkin Elmer). Positive responses were defined as >1,000 counts per min (cpm) with a stimulation index >5 after background subtraction (cpm in wells lacking peptide). Clones were excluded from the analysis if the background count was >1,000 cpm.

Peptide-mapping of antigen-specific $CD4^+$ T cell clones

Antigen-specific $CD4^+$ T cell clones were mapped using a matrix of overlapping HA peptides corresponding to Influenza A California/04/2009, designed using "Deconvolute This!" (Precopio et al., 2008). The matrix consisted of 12 pools with 18 peptides per pool and a coverage of 3. An aliquot of each clone (1.5 × 10^6 cells/mL) was added to the peptide matrix (2 μg/mL) after washing and resting in fresh culture medium without IL-2 for 5 hr. After 3 days, 1 μCi/mL [^{3}H]-thymidine was added to the cultures, and proliferation was measured after 16 hr using a MicroBeta2 Counter (Perkin Elmer). Positive responses were defined as >1,000 cpm with a stimulation index >5 after background subtraction (cpm in wells lacking peptide). Peptide specificity was confirmed similarly using single peptides identified from the matrix responses.

TCR deep-sequencing

Mononuclear cells from matched tonsil and peripheral blood samples were defrosted and rested overnight at 37°C in RPMI 1640 glutamine [-] medium (Invitrogen) supplemented with non-essential amino acids (1%, Invitrogen), sodium pyruvate (1%, Invitrogen), glutamine (1%, Invitrogen), pooled AB human sera (10%, UK National Blood Service), β-mercaptoethanol (0.1%, Invitrogen) and penicillin/streptomycin (1%, Invitrogen). Cells were then surface stained as described above. Among live $CD3^+CD4^+CD45RA^-$ lymphocytes, circulating cells were sorted into cTfh $CXCR3^+$ ($CXCR3^+CXCR5^+PD\text{-}1^+$), cTfh $CXCR3^-$ ($CXCR3^-CXCR5^+PD\text{-}1^+$) and

cNon-Tfh (CXCR5$^-$) subsets, and cells from tonsils were sorted into tTfh GC (CXCR5^{hi}PD-1^{hi}), tTfh CXCR3$^+$ (CXCR3$^+$CXCR5^{int}PD-1^{int}), tTfh CXCR3$^-$ (CXCR3$^-$CXCR5^{int}PD-1^{int}) and tNon-Tfh (CXCR5$^-$PD-1$^-$) subsets. A maximum of 1.2x10^5 cells per subset was sorted using a FACSAria III (BD Biosciences) into RLT buffer (QIAGEN) containing β-mercaptoethanol (10%, Sigma-Aldrich). Sorted cells were stored at –80°C. Each subset from donors 5, 6 and 7 was sorted into two vials for technical replicates (Table S7). Total RNA was isolated using an RNeasy Mini Kit (QIAGEN). Unique molecular identifier (UMI)-labeled 5′-RACE TCRβ cDNA libraries were prepared using a Human TCR Profiling Kit (MiLaboratory LLC). All extracted RNA was used for cDNA synthesis, and all synthesized cDNA was used for PCR amplification. Libraries were prepared in parallel using the same number of PCR cycles and sequenced in parallel using a 150+150 bp NextSeq (Illumina). The total number of reads per subset is shown in Table S8.

TCR sequencing of antigen-specific CD4$^+$ T cell clones

Antigen-specific CD4$^+$ T cell clones were stained as described above for viability and surface expression of CD3 and CD4 (reagent details in Key Resources Table). A maximum of 5 × 10^3 live CD3$^+$CD4$^+$ T cells was sorted into 100 μL of RNAlater (Ambion) using a FACSAria III (BD Biosciences). Sorted cells were stored at −80°C. All expressed *TRA* and *TRB* gene transcripts were amplified using an unbiased template-switch anchored RT-PCR (Quigley et al., 2011). Pure mRNA was isolated from sorted cells using μMACS Oligo(dT) MicroBeads (Miltenyi Biotec), and cDNA was generated using a SmarterRACE Kit (Takara) with Superscript II (Invitrogen). Transcripts were amplified using an Advantage 2 PCR Kit (Takara) with the relevant constant region primers (reagent details in Key Resources Table). Amplicons were separated on agarose gels and extracted using a NucleoSpin Extract II Gel Extraction Kit (Macherey-Nagel). Subclones were generated using a TOPO TA Cloning Kit (Invitrogen) and One Shot Max Efficiency DH5α-T1 Competent Cells (Invitrogen). Conventional sequencing was performed as described previously (Price et al., 2005). Gene use was assigned using the ImMunoGeneTics (IMGT) nomenclature (Lefranc, 2003).

Quantification of influenza-specific IgG

ELISA plates were coated with a commercial Trivalent Influenza Vaccine (0.75 μg/mL, Sanofi Pasteur) or HA protein from Influenza A/California/2009 (2 μg/mL, BEI Research Resources Repository). After overnight incubation at 4°C, plates were washed six times with PBS containing 0.05% Tween-20, blocked with casein (Pierce) for 2 hr at room temperature, and washed again with PBS containing 0.05% Tween-20. Diluted plasma samples (1:500, 1:1,000, 1:2,000 and 1:4,000) were then added in duplicate. After incubation for 2 hr at room temperature, plates were washed again six times with PBS containing 0.05% Tween-20, incubated with alkaline phosphatase-conjugated goat anti-human IgG (1 μg/mL, Sigma-Aldrich) for 1 hr at room temperature, and washed again with PBS containing 0.05% Tween-20. Para-nitrophenylphosphate (Sigma-Aldrich) dissolved at a concentration of 1 mg/mL in diethanolamine buffer (Pierce) was then added for 10 min, and absorbance was read at 405 nm using a Microplate Reader (BioTek) with Open Gen5 software (BioTek). Results were plotted as arbitrary units and standardized against a pool of four plasma samples (Miura et al., 2008).

QUANTIFICATION AND STATISTICAL ANALYSIS

Flow cytometry data

A stop gate was set during acquisition to ensure that the same number of events was acquired and for each sample. Gates were set on the data to determine the frequencies of the different subsets. Analogous subsets were compared between tonsil and peripheral blood using the Wilcoxon matched pairs test. Non-analogous subsets were compared within tonsil and peripheral blood using the Kruskal-Wallis test. *p < 0.05, **p < 0.01, ***p < 0.001, ****p < 0.0001. Boxes show means and quartiles, and whiskers show minima and maxima.

TCR deep-sequencing analysis

A total of 93 × 10^6 TCRβ sequencing reads (up to 8 × 10^6 reads per library) were obtained, from which 1.55 × 10^6 unique UMI-labeled TCRβ cDNA molecules (up to 1.5 × 10^5 molecules per library) were assembled using MIGEC software (Shugay et al., 2014), using a threshold of at least four sequencing reads per UMI. In-frame CDR3β repertoires were extracted using MiXCR software (Bolotin et al., 2015). Each library contained from 500 to 3.5 × 10^4 functional (in-frame, no stop-codons) CDR3β nucleotide clonotypes. Averaged TCR repertoire characteristics weighted by clonotype size (normalized Shannon-Wiener index) were calculated using VDJtools software (Shugay et al., 2015). As the number of cells in the populations sorted from different donors was variable as well as the total reads, the frequency of each clonotype was normalized before analysis to allow an unbiased comparison between diverse subsets. Network analysis was performed using Cytoscape software (https://cytoscape.org). The F2 metric for overlap between two populations was calculated as the sum of the geometric means between the frequencies of shared clonotypes, considering the top2000 clonotypes for each subset. This value was then standardized with the two maximum F2 metrics calculated for the top2000 clonotypes for each of the two populations. F2 metric, % shared clonotypes and diversity indices were analyzed with non-parametric Kruskal-Wallis and Dunn's multiple comparison tests. For each test: *p < 0.05, **p < 0.01, ***p < 0.001, ****p < 0.0001. Linear regression correlations were calculated using the square of the Pearson correlation coefficient (R^2), the slope and the p value of the significance of the difference in the slope from zero (ns = not significant).

Bootstrap method

The complete set of clonotypes was randomly resampled with replacement to obtain two *in silico* replicates of each set of sequences. Using this method, the replicates and the original set had similar distributions, but likely different absolute numbers, for each clonotype. All downstream analyses were performed using the two resampled sets. Linear regression correlations between *in silico* replicates and diversity were calculated using the p value of the difference in the slope from zero.

T cell library analysis

Positive responses were defined as >3,000 counts per min (cpm) with a stimulation index >5 after background subtraction (cpm in the negative control wells). Because $CD4^+$ T cells were seeded at limiting dilution, it was possible to calculate the precursor frequency of responding cells per million according to the Poisson distribution (Campion et al., 2014; Geiger et al., 2009; Lindestam Arlehamn et al., 2013; Mele et al., 2017). The 95% confidence intervals were determined according to the modified Wald method (Harrell, 2001).

Antigen-specific $CD4^+$ T cell frequencies

The frequencies of expanded antigen-specific $CD4^+$ T cell clones were calculated based on the number of clones with confirmed specificity after expansion. Significantly diverse enrichments were identified using Kruskal-Wallis and Dunn's multiple comparison tests were performed. For each test: *$p < 0.05$, **$p < 0.01$, ***$p < 0.001$, ****$p < 0.0001$.

DATA AND CODE AVAILABILITY

MIGEC, MiXCR and VDJtools software are available from MiLaboratory LLC (https://milaboratory.com/software/). The TCR sequencing dataset supporting the current study has been deposited in the Mendeley Dataset repository (https://doi.org/10.17632/wry2ddh8zx.1).